Dipl.-Ing. Elisabeth Hufnagl

# Choice of system neutral treatment and earth fault protection in aged medium voltage cable networks

## DOCTORAL THESIS

to achieve the university degree of

Doktorin der technischen Wissenschaften

submitted to

## Graz University of Technology

Supervisor

Em.Univ.-Prof. Dipl.-Ing. Dr.techn. Lothar Fickert

Professor Matti Lehtonen

Graz, November 2018

# Choice of system neutral treatment and earth fault protection in aged medium voltage cable networks

## Doctoral Thesis

ELECTRICAL
POWER SYSTEMS
TU GRAZ

## Institute of Electrical Power Systems
## Graz University of Technology

### Author
Elisabeth Hufnagl

### Supervising professor
Em.Univ.-Prof. Dipl.-Ing. Dr.techn. Lothar Fickert

### Reviewer
Em.Univ.-Prof. Dipl.-Ing. Dr.techn. Lothar Fickert
Professor Matti Lehtonen

**Head of Department: Univ.-Prof. DDipl.-Ing. Dr.techn. Robert Schürhuber**

**A - 8010 Graz, Inffeldgasse 18-I**
**Telefon: (+43 316) 873 - 7551**
**Telefax: (+43 316) 873 - 7553**
**http://www.ifea.tugraz.at**
**http://www.tugraz.at**

**Graz / November 20, 2018**

TU
Graz

# Acknowledgements

An dieser Stelle möchte ich Herrn Em.Univ.-Prof. Dipl.-Ing. Dr.techn. Lothar Fickert für die Bereitschaft zur Betreuung meiner Arbeit danken.

Ein großer Dank gilt auch Herrn Univ.-Prof. DDipl.-Ing. Dr.techn. Robert Schürhuber, der mir in seiner Funktion als Institutsleiter die für die Erstellung einer Dissertation nötigen Freiheiten einräumte und somit beste Rahmenbedingungen für die Fertigstellung gewährleistete.

Besonders möchte ich mich bei Prof. Matti Lehtonen bedanken, der sich bereit erklärt hat, diese Arbeit zu begutachten.

Auch möchte ich mich bei meinen lieben Kollegen und Kolleginnen am Institut bedanken. Es sind nicht zuletzt zahlreiche Diskussionen und wohlwollend formulierte Kritik, die eine Arbeit voranbringen und manches Mal Anstoß zu neuen Ideen geben.

# Abstract

The aim of this thesis is to address reliability and protection issues arising with considerations concerning a change in neutral point treatment.

Starting with assessment criteria for protection schemes of aged urban medium voltage networks, possible reasons and boundary conditions for a change in system neutral treatment are discussed.

Concerning earth fault protection structures, this thesis reviews state of the art earth fault protection methods and assesses possible limitations to the respective method. A particular focus lies on the active residual current method using high detection currents, specifying an engineering approach to the electric and thermionic dimensioning of system neutral resistors.

In the course of risk assessment, cross-country-faults as impact factors on network reliability and monetary considerations are discussed. The influence of line-to-ground faults and subsequent double earth faults in combination with resonant grounding and aged cable network structures on the network reliability is assessed, using an approach which is independent from network calculation software. The results are compared with an equivalent assessment for the same network structure with low ohmic neutral earthing. The method described in this thesis reduces a complex problem with a considerable number of impact factors to a simplified evaluation, which allows - based on an adequate choice of input parameters - realistic estimations. By varying network specific input parameters, the respective parameter's impact on the earth fault induced non-availability is assessed. Furthermore recent developments in standardisation concerning personal and technical risk and safety issues are addressed.

**Keywords: system neutral treatment, earth fault, earth fault detection, protection structures, medium voltage networks, aged cable networks, reliability**

# Kurzfassung

Diese Dissertation greift Fragestellungen aus dem Bereich der Netz-Zuverlässigkeit und der Schutztechnik auf, die im Zuge von Voranalysen betreffend möglicher Sternpunktumstellungen auftreten können.

Mit schutzbezogenen Bewertungskriterien zu gealterten städtischen Mittelspannungsnetzen beginnend, werden mögliche Gründe und Randbedingungen für eine Sternpunktumstellung behandelt.

Sternpunktumstellungen ziehen üblicherweise Anpassungen oder Umstellungen des Erdschluss-Schutzes nach sich. Derzeit gängige Erdschluss-Schutz und -Ortungs-Methoden und deren Grenzen werden in dieser Arbeit evaluiert. Besonderes Augenmerk wird hierbei auf (stromstarke) Wattreststrom-Verfahren gelegt. Für die Auslegung des notwendigen Widerstandes werden sowohl für die elektrische, als auch für die thermische Dimensionierung, Richtlinien angegeben.

Die Risikobetrachtungen beschäftigen sich mit dem Einfluss des Doppelerdschlusses auf die Netz-Zuverlässigkeit sowie auf finanzielle Aspekte. Die Auswirkung von Erdschlüssen und Folgefehlern in Form von Doppelerdschlüssen in gealterten urbanen Mittelspannungsnetzen, die gelöscht betrieben werden, wird mit einem von Netzberechnungsprogrammen unabhängigen Ansatz untersucht. Die erzielten Ergebnisse werden mit jenen eines niederohmig geerdeten ansonsten ident aufgebauten Netzes verglichen. Die in dieser Arbeit beschriebene Methode erlaubt - sinnvoll gewählte Eingangsparameter vorausgesetzt - realistische Abschätzungen. Durch das Variieren netzspezifischer Eingangsdaten, wird deren Einfluss auf die erdschlussbedingte Nichtverfügbarkeit ermittelt. Weiters werden aktuelle Entwicklungen in der Normung bezüglich Erdung und Personenschutz aufgegriffen.

**Schlüsselwörter: Sternpunktbehandlung, Erdschluss, Erdschluss-Ortung, Schutztechnik, Mittelspannungsnetze, Zuverlässigkeit, gealterte Kabelnetze**

# AFFIDAVIT

I declare that I have authored this thesis independently, that I have not used other than the declared sources/resources, and that I have explicitly indicated all material which has been quoted either literally or by content from the sources used.

Ich erkläre an Eides statt, dass ich die vorliegende Arbeit selbstständig verfasst, andere als die angegebenen Quellen/Hilfsmittel nicht benutzt, und die den benutzten Quellen wörtlich und inhaltlich entnommenen Stellen als solche kenntlich gemacht habe.

Graz, November 20, 2018

Elisabeth Hufnagl

# Contents

# Acronyms

**ALARA**    As Low As Reasonably Achievable

**ASIDI**    Average System Interruption Duration Index

**ASIFI**    Average System Interruption Frequency Index

**BNetzA**    Bundesnetzagentur

**CAIDI**    Customer Average Interruption Duration Index

**CB**    Circuit Breaker(s)

**CENS**    Cost of Energy not Supplied

**CI**    Customers Interrupted

**CIC**    Customer Interruption Cost(s)

**CRF**    Coincidence Reduction Factor

**DMT**    Definite Time-delay Overcurrent Release

**DSO**    Distribution System Operator(s)

**e/f**    earth fault

**ENS**    Energy Not Supplied

**EPR**    Earth Potential Rise

**HV**    High Voltage

**HPE**    Healthy Phase Earthing

**IEEE**    Institute of Electrical and Electronics Engineers

**LONE**    Low Ohmic Neutral Earthing

**LV**    Low Voltage

**MF**    Monetary Factor

**MV**    Medium Voltage

**OHL**    Over Head Lines

**p.u.**    per unit

| | |
|---|---|
| **RG** | Resonant Grounding |
| **RMU** | Ring Main Unit(s) |
| **SAIDI** | System Average Interruption Duration Index |
| **SAIFI** | System Average Interruption Frequency Index |
| **STLONE** | Short Time Low Ohmic Neutral Earthing |
| **TSO** | Transmission System Operator |
| **VOLL** | Value of Lost Load |
| **XLPE** | Cross Linked Polyethylen |

# 1 Introduction

Due to utmost demands concerning reliability and power quality, neutral point treatment increasingly gains interest. The shift to new strategies in power system planning causes a re-evaluation of impact factors on technical and economic grid design. A risk-based approach can be used to compare network expansion scenarios, restructuring measures or even changes in neutral point treatment. The expression risk applies to technical, economic as well as to personal risks (in terms of personal safety).[1] Taking the possibility of future penalty structures into account, costs caused by reinforcement of the electric network should be compared to follow-up costs of interruptions (e.g. customer interruption costs, penalties). Thus anticipatory investment strategies can be developed.

## 1.1 Motivation

In Austria as well as in Germany the resonant earthed neutral is the most common neutral point treatment of medium voltage networks, regardless of the dominating characteristics of the particular network. In the course of the past years, power system engineering experienced several changes of perspective and planning principles. Among other things, the common limit of grid expansion, given by the self-extinguishing current is being replaced by a more individual approach of assessing the touch- and step voltage of facilities. Therefore, grid expansion is no longer limited by the line capacitance, which gains even more importance with the growing percentage of cable in network structures.

Moreover, the resonant earthed neutral becomes less and less indispensable as an increasing frequency of cable joint defects, caused by voltage stress on aged isolation, forces Distribution System Operator(s) (DSO) to interrupt the affected network branch for instance during an earth fault (which would raise the line-to-ground-voltage of the remaining network, while its operation is continued). As the interruption frequency rises, non-availability significantly grows for the affected stations as well as for the customer, even though the overall network is still operated during earth faults. On the downside, as a consequence of instant interruption of earth faults through the DSO, customers who run a network (for instance industrial networks) don't get the chance to complete earth fault detection in time. Hence the question arises, if the resonant earthed neutral actually is the most suitable neutral point treatment for aged urban medium networks. This thesis is meant to define the framework for several neutral point treatments on urban medium voltage networks.

---

[1]Risk is defined as the product of the probability and the damage

## 1.2    Objective

The thesis's main objective is:

- to show the relations between system neutral treatment and reliability quantities for aged medium voltage cable networks

- to research decision criteria for the choice of system neutral treatment and the subsequent choice of earth fault protection structure

- to research earth fault protection structures and their application

    - design process

    - technological necessities

- to show economic advantages of changes in the system neutral treatment - earth fault protection respectively - regarding possible incentive based regulatory regimes

## 1.3    Scope of Research

Explicitly exempted objectives ("non-goals"):
This thesis does not provide

- analyses of earth fault detection or localization algorithms

- analyses for networks dominated by Over Head Lines such as rural network areas or industrial networks

- optimization approaches to switching or distribution automation

## 1.4    Scientific Contribution

During the work with the Institute of Electrical Power Systems, the following publications were authored or decisively contributed to:

---

## Focus on subjects linked to the PhD thesis

[1] "The compliant integration of (renewable) power sources in MV or LV grids and the impact on grid reliability", in 2015 International Conference on Renewable Energy Research and Applications (ICRERA), 2015

[2] "Evaluation of an urban medium-voltage network by using reliability indices", in ELEKTROTEHNIŠKI VESTNIK, Journal of Electrical Engineering and computer Science, 2016

[3] "A simplified procedure to determine the earth-fault currents in compensated networks", in ELEKTROTEHNIŠKI VESTNIK, Journal of Electrical Engineering and computer Science, 2016

[4] "Erdschlussbehandlung unter regulatorischen Aspekten", in ETG-Fachbericht 151, 2017

---

## Other publications[2]

"Auswirkungen von Umstrukturierungsmaßnahmen auf die Zuverlässigkeitskennzahlen in einem städtischen Mittelspannungsnetz", in Energiesysteme im Wandel: Evolution oder Revolution?, 2015

"Reflections on global earthing systems", Komunalna Energetika - Power Engineering, 2015

"Efficient calculation of earth fault currents in compensated networks", Komunalna Energetika - Power Engineering, 2015

"Kritikalität der Parallelführung eines 110-kV-Netzes mit einem MS-Netz und der Einfluss der Nichtlinearität der Petersenspule", 14. Symposium Energieinnovation, 2016

"Ausgewählte elektrotechnische Aspekte zu urbanen Seilbahnen", in Österreichische Zeitschrift für Verkehrswissenschaft, 2017

---

[2]Selection of publications. For full list, see `https://graz.pure.elsevier.com/en/persons/elisabeth-hufnagl/publications`

Elisabeth Hufnagl

## 1.5 State of the Art

Generally, the standard neutral point treatment of medium voltage networks in Austria (as well as in Germany) is the resonant grounding.

A typical protection scheme for a medium voltage network which is dominated by cable, is described in [5] and [6] as follows:

- Overcurrent protection via DMT in every feeder

- DMT with one zone dedicated to earth fault in incoming feeders

- Earth fault protection in every outgoing feeder

The transformers in this network are protected by the use of:

- Differential protection with additional earth fault differential protection on the medium voltage side (restricted earth fault)

- DMT in the transformer neutral (in case of tripping, the transformer is switched off, to avoid operation with an isolated neutral point)

- Possibly thermal overload protection in the neutral point

While in northern countries such as Finland, DSO think about switching the neutral point treatment of their medium voltage networks to resonant grounding [7], system operators of aged, cable dominated, medium voltage networks in Austria as well as in Germany discuss the benefits of the low-resistance neutral point treatment. The main reason for that is the steep rise of cable joint outages due to continued operation during earth faults.

In the following sections, state of the art earth fault detection schemes are described. A more detailed description, as well as technical requirements, is given in section 4.2. A helpful summary of earth fault localization methods is given in e.g. [8]. A very detailed work on the topic of earth fault detection and localization with a focus on transient earth fault was published by Gernot Druml in [9]. A more recent work on this topic with a focus on high ohmic transition impedances is [10].

### 1.5.1 Resonant Grounding

By using an arc-suppression coil, the earth fault current is nearly compensated. Just a small percentage of inductive current remains as a result of detuning. This makes sure, the 50-Hz-fundamental of the current remains on the overcompensated side of the V-curve (see Figure 1). As a result, possible changes in

the network configuration, leading to an inevitable change of capacitive current, don't cause an immediate danger of resonance. Therefore, undesirable high voltages on the arc-suppression coil are prevented. Further information on resonant grounding and specific research on the topic of detuning, asymmetry by capacitive influence and extension reserve can be found in [11] and [12].
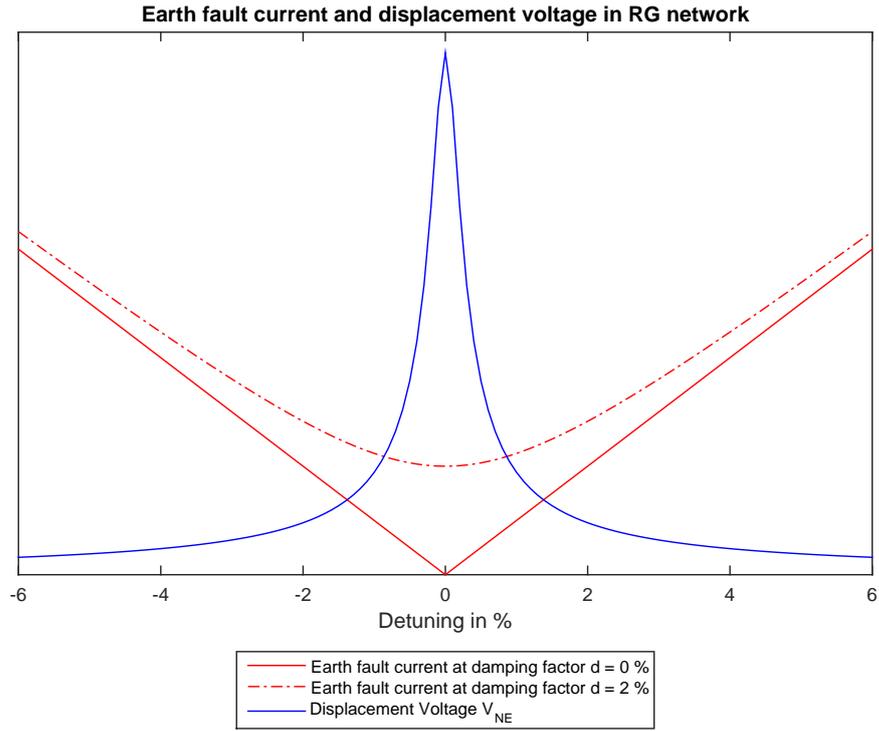


Figure 1: Exemplary diagram of earth fault current and displacement voltage over detuning

Detuning is defined as the deviation from total compensation as described in Equation 1.

$$\nu = \frac{I_L - I_C}{I_C} = \frac{\dfrac{1}{\omega \cdot L_{Pet}} - \omega \cdot \sum C_E}{\omega \cdot \sum C_E} = \frac{1}{\omega^2 \cdot L_{Pet} \cdot \sum C_E} - 1 \qquad (1)$$

$\nu$          detuning

$I_L$         inductive current caused by the arc-suppression coil

$I_C$         capacitive current

$L_{Pet}$     inductance of the arc-suppression coil (Petersen coil)

$\sum C_E$    total of network capacitances

The Resonant Grounding (RG) network is considered overcompensated if the resulting earth fault current is inductive and undercompensated if the resulting earth fault current is capacitive.

The damping is defined by the active power losses of the arc-suppression coil. Equation 1 shows the relevant relations. In [12] an in-depth derivation for the calculation of the damping from network characteristics is presented.

$$d = \frac{I_{act}}{I_C} \tag{2}$$

$d$        damping, occasionally referred to as $\delta$

$I_{act}$        active current caused by the active power losses of the arc-suppression coil

$I_C$        capacitive current

The displacement voltage $V_{NE}$ can be calculated using Equation 3.

$$V_{NE} = \frac{V_{ij}}{\sqrt{3}} \cdot \frac{k}{\sqrt{\nu^2 + d^2}} \tag{3}$$

$V_{ij}$        line-to-line voltage

$k$        capacitive unbalance, see Equation 4

$\nu$        detuning

$d$        damping, occasionally referred to as $\delta$

$$k = \frac{C_{1E} + \underline{a}^2 \cdot C_{2E} + \underline{a} \cdot C_{3E}}{C_{1E} + C_{2E} + C_{3E}} \tag{4}$$

$C_{iE}$        line-to-gound capacity of the respective line i

$\underline{a}$        operator which enables a rotation by $e^{j\frac{2\pi}{3}}$

In [11], the capacitive unbalance , as well as its assessment from earth fault experiments, is discussed in detail.

### 1.5.2 Earth Fault Treatment: DMT as main Protection Device

Apart from the use of earth fault detection relays using specialized algorithms for the detection and localization of line-to-ground faults, it is possible to rely entirely on overcurrent protection in the form of DMT.

### 1.5.3 Earth Fault Treatment: Additional Grounding of the Affected Phase

This method is used in compensated networks, for the forced elimination of the earth fault current. It is more of an earth fault treatment than an earth fault detection or localization method. Nevertheless, it contributes to a more complete review in this section.

The additional grounding of the affected phase creates a parallel path for the current within the Medium Voltage (MV) substation. In [13] the risk of hazardous touch voltages on the neutral conductor of the Low Voltage (LV) network due to this earth fault protection method is evaluated. The authors claim, that even though theoretic analysis implies negative influences of a shunting resistor on the earth fault current, several experiments in an urban MV distribution network do not confirm this assumption. Furthermore, they emphasise the missing increase of touch voltage the absence of EPR, even though experiments where conducted with very low resistance (basically solid grounding of the affected phase). This is influenced by the sound grounding system.

### 1.5.4 Earth Fault Detection Methods: Harmonic Components

Depending on the harmonic distortion of the network, this system can be applied by using natural harmonics, measuring the 5th harmonic, or, if available, forced harmonics, by injecting a defined signal using audio frequency remote control. There are basically three procedures for earth fault detection with harmonic components:

- $sin(\varphi)$ procedure: the significant property is the angle between the 5th harmonic of the earth fault current and the displacement voltage, which is between the transformer neutral and ground.

- Comparative evaluation based on the current: the significant property is the magnitude of the earth fault current, which is compared to the current in the healthy network branches.

- Evaluation based on the magnitude of the current: the significant property is the magnitude of the 5th harmonic of the earth fault current. (Not recommended)

As shown in Figure 2, in resonant grounded networks the harmonic components of the earth fault current flow via the fault impedance $Z_F$ ($Z_F$ can be assumed ohmic, as it is dominated by thermic effects) and the faulty phase, rather than

the Petersen coil, as the inductance increases its impedance with the order of the harmonic. Therefore, the capacities of the healthy phases discharge themselves, producing a capacitive current which flows back to the transformer neutral via the faulty phase. As a consequence, the earth fault afflicted phase can be distinguished from the healthy ones by its distinct magnitude. Usually the 5th harmonic is used, as it is the strongest harmonic in distribution systems. Nevertheless it may occur, that the harmonic distortion is not sufficient for the use of natural harmonics. In this case, audio frequency remote control can inject forced harmonics into the network.
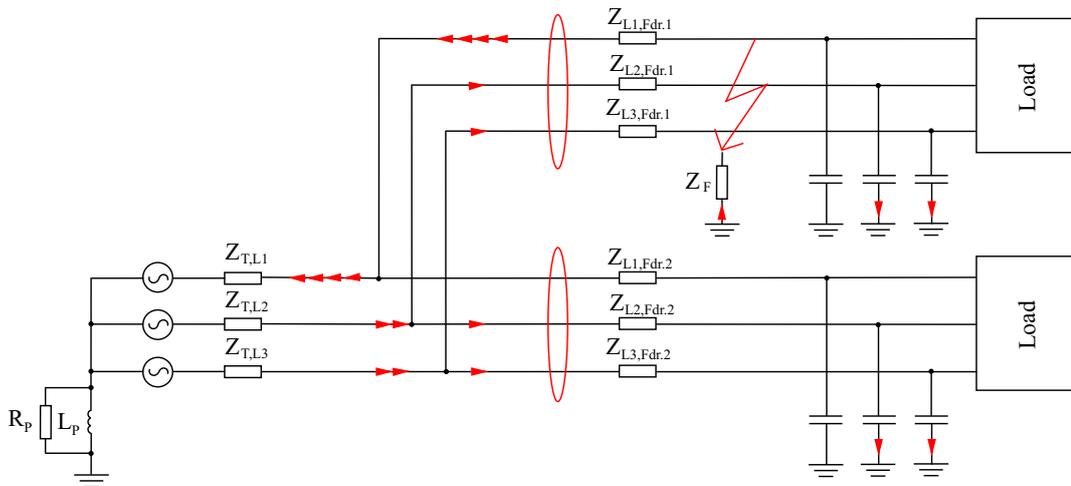


Figure 2: Earth fault detection using harmonic components, [9]

### 1.5.5 Earth Fault Detection Methods: Active Residual Current

This detection method uses the active residual current component of the earth fault current. As shown in Figure 4, the healthy phases are sources of a capacitive current, which flows to the transformer neutral. While the faulty phase's reactive current is compensated to a certain percentage (detuning of the arc-suppression coil), the active current remains. Therefore, it can be used for earth fault detection purposes. The main idea is to use the angle ($\varphi$) between the earth fault current and the displacement voltage over the transformer neutral (see Figure 3). A deviation from the ninety degree angle between the measured current ($I_{Fdr}$) and the displacement voltage ($V_{NE}$) indicates the faulty feeder.
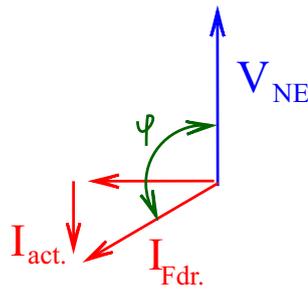
Figure 3: Relations between the active residual current, the displacement voltage and the angle

For this method, it is possible to use the active residual current as it is given by the network characteristics, or to increase the current via the following measures:

- Parallel resistance connected to Petersen coil, as shown in Figure 4

- Short Time Low Ohmic Neutral Earthing (STLONE)

- High current short time low ohmic neutral earthing

- Healthy Phase Earthing (HPE)

While the first three methods interfere with the transformer neutral, the HPE method works slightly different but still increases the active residual current. Basically for HPE a resistor is used, to connect a healthy phase to ground. In doing so a high current is achieved without putting thermic stress to the transformer neutral. The obtained current is especially easy to detect and measure. A detailed description of the method and its theoretical background is given in section 4.2.4.
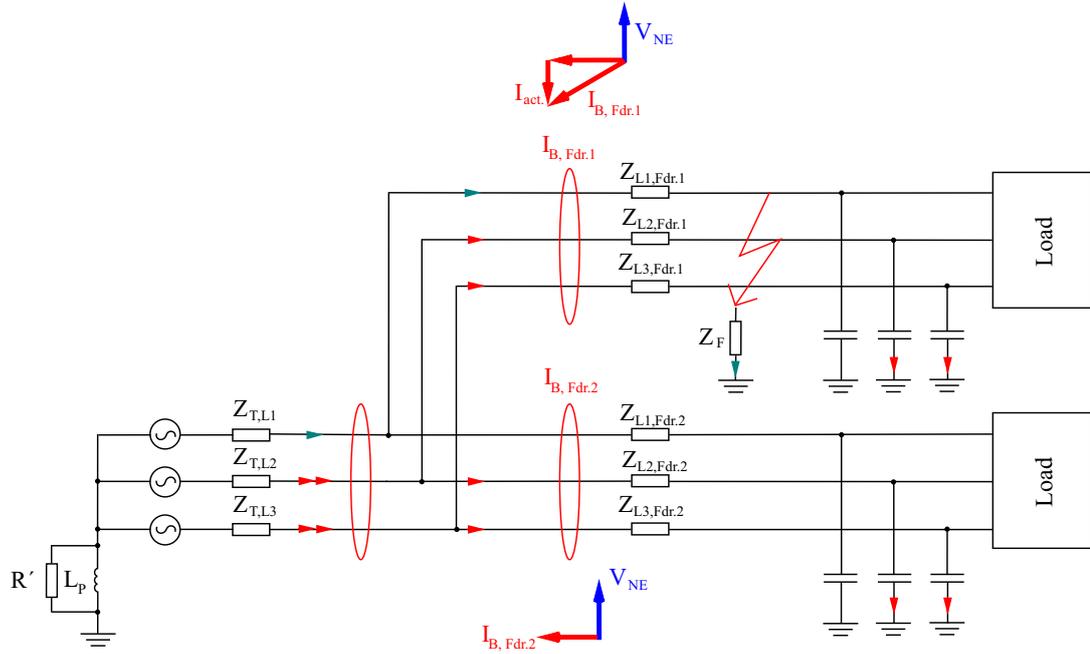
Figure 4: Earth fault detection using the increased active residual current, [9]

Depending on the choice of detection method, the resulting active residual current reaches the kA-region. A more detailed description of the functionality and the equipment needed is given in section 4.2.3 and section 4.2.4.

### 1.5.6 Earth Fault Detection Methods: Pulse Method

In order to achieve a detectable, recognizable detuning of the earth fault compensation, a capacitor is connected parallel to the auxiliary winding of the transformer in a defined pulse pattern. As a result, the degree of overcompensation is decreased while the capacitor is connected to the auxiliary winding. The resulting earth fault current decreases with the degree of detuning $\nu$. According to [9], the change of reactive current should be around 2 to 3 percent of the line-to-earth-capacity of the network. The pattern can be recognized between the pulse generator and the earth fault location.
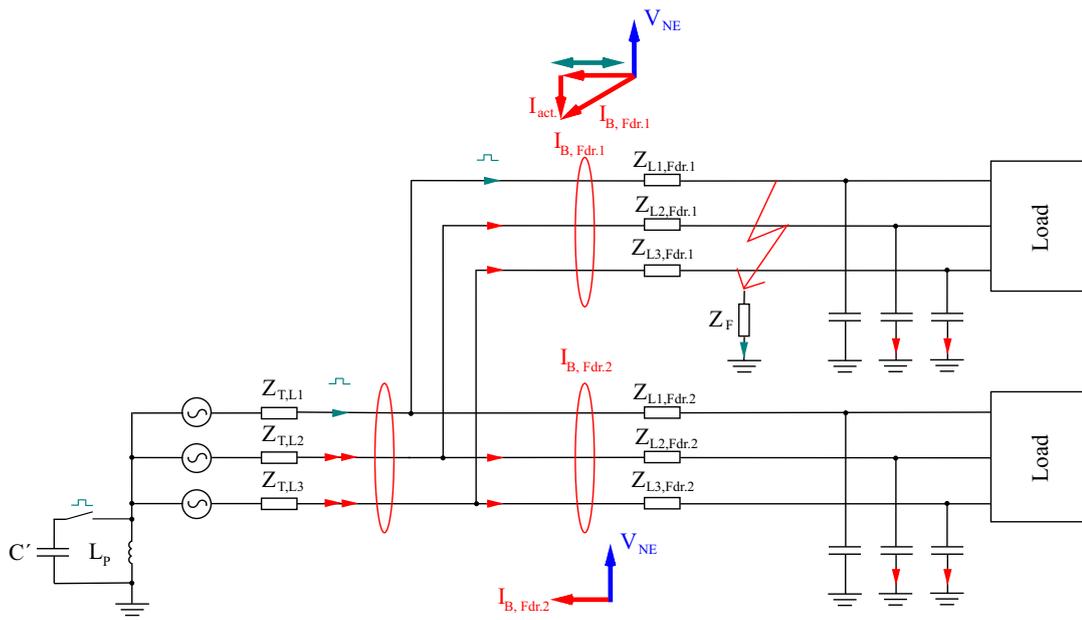
Figure 5: Earth fault detection using the pulse method, [9]

## 1.6 Research Questions

1. Can a change in system neutral treatment contribute to a decrease in interruption frequency?

2. Is the average system non-availability of urban cable networks significantly affected by a prospective change in system neutral treatment?

3. Can the contribution of a prospective change in system neutral treatment in urban cable networks be evaluated by the means of probabilistic reliability calculation?

4. Which aspects influence the choice of system neutral treatment in MV cable structures?

5. Which network structures benefit from a change in system neutral treatment?

6. Which technological changes are necessary in the course of a change in neutral point treatment?

7. Which aspects of the earth fault protection scheme have to be reassessed in the course of a change in system neutral treatment?

8. Which factors limit the active residual current method - in terms of (safety) standards as well as in terms of technical limits?

9. Can the minimum lag time of system neutral resistors be estimated by simple models?

10. Are there economic advantages of change in system neutral treatment concerning incentive based regulatory regimes?

## 1.7 Outline of this Thesis

In order to provide a starting point, a typical urban cable network is described in section 2. Besides an example of an urban network and its protection structure, a summary of various studies on damage rates of equipment parts, with a focus on cables and cable accessories is provided.

In order to answer the research questions concerning the choice of system neutral treatment - possible motivation, technical reasons, intended results - as well as induced consequences, limitations and potential side-effects are discussed in section 2.3. The findings of this section are summarised in a flow chart, designed to

guide through the decision process.

In section 3, one method of probabilistic reliability assessment is proposed. The advantages and disadvantages of the approach are discussed, including the reasons for a change of method in order to answer the research questions dealing with reliability assessment and network evaluation.

In section 4 specifics to earth fault detection systems including cost factors and design requirements are summarised.

In section 5 the theoretical background to the assessment of thermic stress as well as three approaches to an estimation of the heating behaviour (cooling behaviour respectively) of the system neutral resistor in high current earth fault detection methods are presented.

Selected aspects of risk assessment are discussed in section 6.

# 2 Assessment Criteria for Protection Schemes

The choice of sustainable protection schemes depends on several aspects, which are discussed in this chapter.

- Expansion of the network (see section 2.1)

- Percentage of cable in the network

- Plans concerning network extension

- General structure such as open ring-structure, radial distribution structure, existing protection scheme

- Additional impact factors such as old cable structures, aged cable joints, existing problems concerning dielectric strength (see section 2.2)

## 2.1 Network Characteristics and Protection Requirements

The sum of Austrian MV networks reached 69062 kilometres of system length by the end of 2016. The percentage of underground cables lies at around 62 percent of the total MV system length. [14]
The share of cables in Austrian MV networks varies from network to network, as the electrical infrastructure often depends on the degree of urbanisation. While rural regions are mainly supplied by Over Head Lines (OHL), densely populated areas obtain electricity by cable networks. In section 2.1.1, a realistic urban network structure is described.

### 2.1.1 Expansion and Structure of Urban Medium Voltage Networks

An existing urban MV network is described in [5] and [6] as follows:

- 860 km of system length - 98 percent consist of cables

- open ring structure

- 10 stations per feeder (semi-ring respectively)

- 20 arc-suppression coils

- 9 substations - 8 substations are grounded via grounding transformer

- 1450 short circuit indicators (not all of them are connected to control center)

According to [5] this network meets the requirements given in DIN VDE 0101 concerning touch voltages unless the switching time exceeds one second. The change in neutral point treatment of this network from resonant grounding to Low Ohmic Neutral Earthing (LONE) cuts the costs in half. The reason for this

is the need of enforcements concerning the arc-suppression coil as well as the earthing system in case of a further use of resonant grounding.

### 2.1.2 Autorecloser and Selective Disconnecting

One major impact factor on network reliability is the level of automation within the distribution network. As stated in [15], the implementation of distribution automation to a greater extent allows a reduction of customer minutes lost by two thirds. A quite similar result was achieved in [1] (author's contribution), were the non-availability was reduced by fifty percent, simply by replacing certain locally switched Circuit Breaker(s) (CB) by remote controlled CB and therefore significantly reducing travelling time for technicians.

Also a strong relation between the customer damage (which might be interpreted as Customer Interruption Cost(s) (CIC)) and the optimum number of automated switches is identified. This is caused by the fast restoration of service for intact network segments within minutes, while manual switching actions may take up to one hour or even longer due to long distances or traffic. Still there is no clear advantage in automated switching for unknown fault locations. Therefore, an accurate fault detection system is required to fully benefit from distribution automation. Furthermore, a focus on automated switching in inner city areas, instead of placing them evenly distributed in the entire grid, is the most beneficial scenario. [15]

Even though the implementation of fully automated switching or remote controlled CB appear quite promising, for some urban cable networks it is not as highly prioritised as the change in neutral point treatment in order to improve network reliability. This may be caused by the lack of advantage in terms of vague fault localisation and detection.

## 2.2 Damage Rates of Equipment Parts

In this subsection the findings of [16] are summarised. The damage rates for equipment parts described in [16] mainly come from [17].

The reliability of a MV network is strongly influenced by its damage rates. Most equipment parts used in energy supply networks tend to reach long life cycles. During these long periods of operation, the material is bound to age at a certain rate. Depending on the loading of the equipment parts the ageing process may be accelerated, as higher voltages strain the dielectric strength and high currents increase the thermal stress.

The author of [16] proposes a risk based optimisation of maintenance and repair of MV cables, in order to achieve a maximised operation duration while minimising unplanned interruptions due to aging-related cable damage. According to [16] the aging-related damage rate of Cross Linked Polyethylen (XLPE) cables follows an exponential function (see Equation 5).

$$\lambda_{aging}(t) = a \cdot e^{b \cdot t} \tag{5}$$

$\lambda_{aging}$      aging-related damage rate

$a$      parameter for calculation of aging-related damage rate

$b$      parameter for calculation of aging-related damage rate

$t$      time

The parameters $a$ and $b$ in Equation 5 depend on the type of tripping as well as on the generation of XLPE cable. [16] distinguishes between fully automated switching actions by protection devices and manual switching actions with time lags. There is also a difference between XLPE cables of the "old" (laid until the mid-eighties) and the new generation. Comparing Figure 6 and Figure 7, it becomes clear, that the function describing the damage rate of the cable generation laid until the mid-eighties experiences a significantly steeper rise of damages over the years.
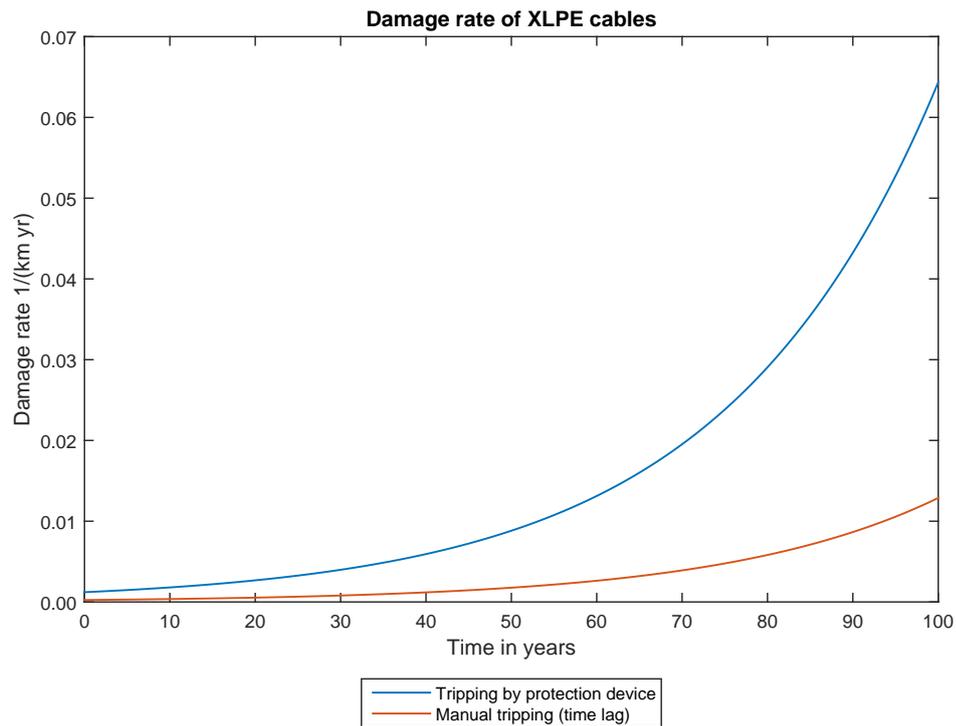
Figure 6: Damage rate of XLPE cables, with parameters from [16]
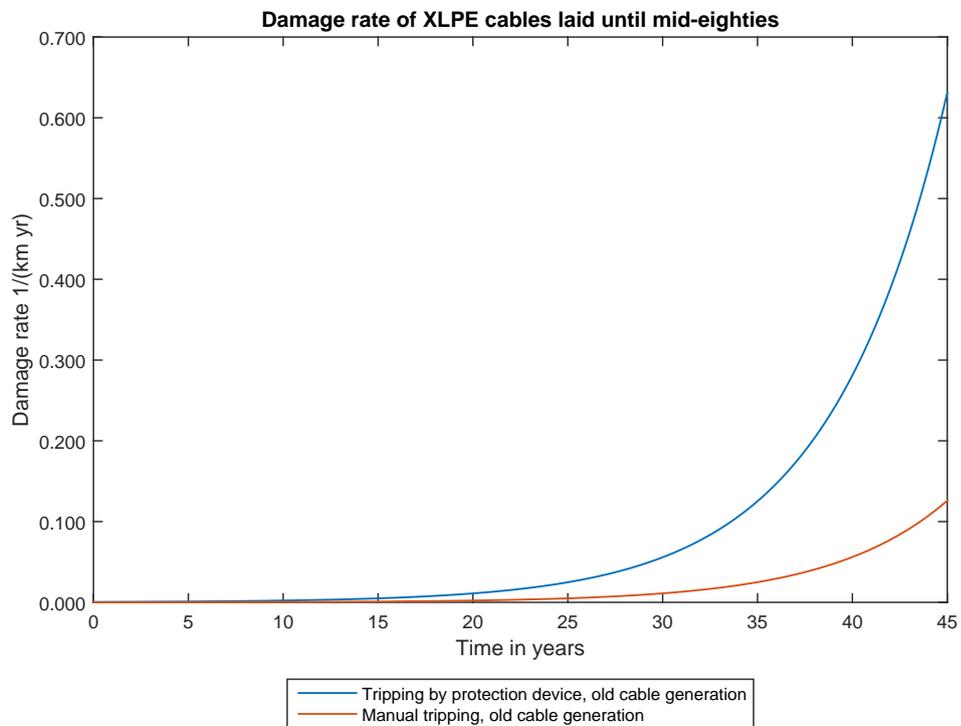


Figure 7: Damage rate of XLPE cables of the old generation, with parameters from [16]

The damage rate of metal-sheathed cables is considered to be constant. While the rate of automated switching actions is assumed to be 0.00408 per kilometre and year, the manual switching is assumed to be 0.0024 per kilometre and year. The author of [16] also quotes damage rates of cable joints and terminations from [17] (see Table 1). Once more the damage rate is assumed to be constant. The damage rate is still in reference to the cable length and there is no distinction between joints and terminations.

Table 1: Damage rates of cable joints and terminations, [16][17]

|  | Automated tripping rate by protection device in $\dfrac{1}{km \cdot yr}$ | Manual tripping rate in $\dfrac{1}{km \cdot yr}$ |
|---|---|---|
| XLPE cables | 0.001127 | 0.000397 |
| Metal-sheathed cables | 0.007816 | 0.001090 |

Some assumptions lead the author of [16] to a damage rate of cable joints as shown in Table 2.

Table 2: Damage rates of cable joints according to [16]

|  | Automated tripping rate by protection device in $\dfrac{1}{yr}$ | Manual tripping rate in $\dfrac{1}{yr}$ |
|---|---|---|
| XLPE cables | $2.47 \cdot 10^{-4}$ | $8.69 \cdot 10^{-5}$ |
| Metal-sheathed cables | $1.71 \cdot 10^{-3}$ | $2.39 \cdot 10^{-4}$ |

A publication on the quality and condition of MV cables and cable accessories (see [18]) gives an overview on fault rates for several countries and cable types. For example, it distinguishes the origin of faults in cable lines in Helsinki for the years between 2004 and 2010 as follows:

- Cables: 41%

- Joints: 38%

- Terminals: 21%

For the same years of operations [18] provides fault rates of different cables in Helsinki's MV network (see Table 3):

Table 3: Fault rates of Helsinki's MV cables between 2004 and 2010, [18]

| MV cable type | Fault rate in $\dfrac{1}{100km}$ |
|---|---|
| XLPE cable | 0.4 |
| Oil-paper cable (APYAKMM) | 2.4 |
| Oil-paper cable (PYLKLJ/PLKVJ) | 9.2 |

In [18] also a summary of several cable systems from different countries (see Table 4) is given. The author quotes several sources which are listed in this work as [19], [20],[21], [22] and [23].

Table 4: Fault rates of several MV cable systems, as found in [18] (see also in [19, 20, 21, 22, 23])

| MV cable type | Fault rate in $\frac{1}{100km}$ |
|---|---|
| Helsinki 2004-2015 all types | 0.9 |
| Sweden 2003-2007 all types | 2.0 |
| Denmark oil type 1998-2007 | 2.4 |
| Denmark XLPE 1998-2007 | 0.6 |
| Portugal oil type 2001-2013 | 4.7 |
| Portugal dry type 2001-2013 | 3.2 |
| USA before 1998 all types | 4.3 |
| USA, all types 2006-2007 | 7.5 |

## 2.3 Choice of Neutral Point Treatment and Earth Fault Protection Scheme

As stated in the beginning of this chapter, the choice of protection scheme depends on several aspects. The actual neutral point treatment is a further limitation criteria concerning the schemes to choose from. In Figure 8, the relations and correlations between neutral point treatment and earth fault protection are briefly outlined.
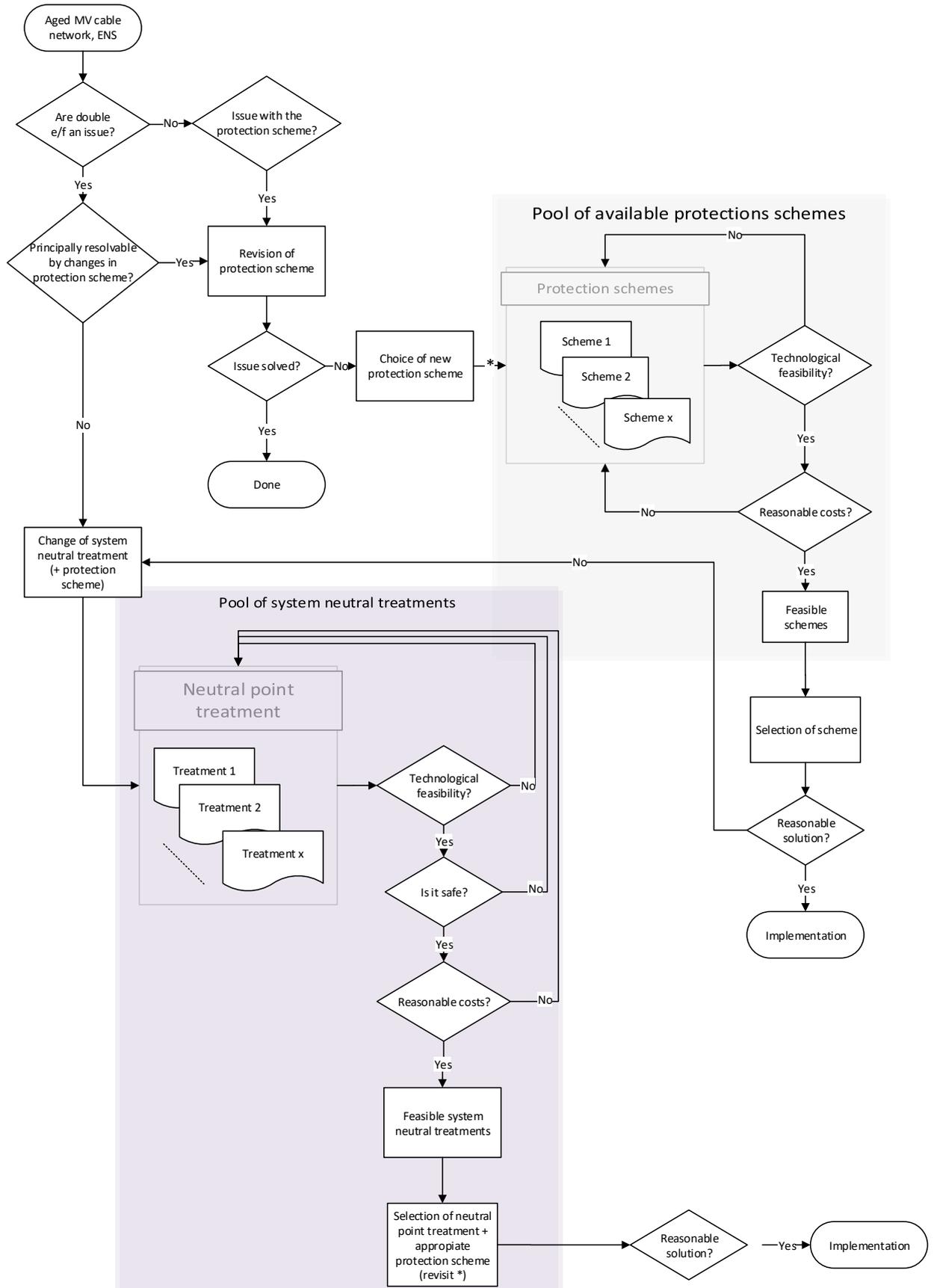
Figure 8: Choice of earth fault protection structure for MV cable networks

In Table 5 an overview on the findings of this chapter is given. The solidly grounded system neutral is not listed below, as it is covered by Low Ohmic Neutral Earthing. Solidly grounded system neutrals are not common in urban MV networks. For detailed descriptions see section 2.3.2 and section 4.

Table 5: Earth fault protection structures depending on the neutral point treatment

|  | isolated network | low ohmic neutral earthing | resonant grounding |
|---|---|---|---|
| harmonics | ✓[51] | ∼ | ∼ |
| $sin\varphi$ | ✓ | ∼ | ✓ |
| $cos\varphi$ | − | ✓ | ✓[52] |
| Short Time Low Ohmic Neutral Earthing | − | not necessary | ✓[53] |
| Healthy Phase Earthing | − | not necessary | ✓[54] |
| pulse method | − | − | ∼ (with limitations)[55] |

### 2.3.1  Choice of Neutral Point Treatment

Decision criteria for the choice of neutral point treatment[3]:

1. Network expansion

   The expansion of the network is one impact factor to be considered, as the system length defines the capacitive current which has to be interrupted or compensated. One of the decision criteria for a certain neutral point treatment is the actual network expansion; to be more precise: the system length and share of cables. As with increasing system length, the capacitive current increases, there is due to limitations of self-extinguishing (for OHL sections) as well as step- and touch voltages a maximum current set to achieve a limited reactive residual current during earth faults.[4] Thus for

---

[51]criterion: degree of harmonic distortion

[52]criterion: angle between the displacement voltage and the active residual current

[53]design parameters: design current, system neutral resistance

[54]design parameter: design current, system neutral resistance

[55]advised for strictly radial or open ring structures; work around option for closed ring structures

[3]The decision criteria given in the list is enumerated solely for structure purposes. There is no intention to prioritize the given aspects. Also this list is not exhaustive.

[4]The network's ability to self-extinguish earth fault currents basically means the electric arc in the actual fault location extinguishes without external force.

networks with isolated neutral points the network expansion is limited too in order to heed limitations to permissive touch voltages and arc-suppression. Through the use of Petersen coils, the residual current is reduced to a level to be defined during the design process. A main origin of the active residual current is the arc-suppression coil. By means of material and design the active power losses of the coil can be influenced, possibly entailing higher costs. Even though the main goal of Resonant Grounding (RG) is the compensation of the earth fault current, the arc-suppression coil is usually detuned to a certain percentage.

2. Limit to the self-extinguishing current
   A certain limit to the self-extinguishing current used to be a significant network planning aspect. By now, the design process gradually shifts towards the resulting fault current as well as admissible step- and touch voltages.
   As for networks with isolated neutral point, aside from network expansion, no further influence on the resulting earth fault current is given, the limit to the self-extinguishing current is even smaller than the limit to networks with RG. For networks with RG, the resulting current is defined by the degree of detuning, which is chosen during the design process.

3. Nominal voltage and over-voltage stress
   The nominal voltage influences the choice of neutral point treatment, as proper insulation by means of material, as well as distances becomes more difficult to achieve with increasing voltages. As a consequence, for High Voltage (HV) networks solid grounding is the neutral treatment of choice, as elevated voltages due to network faults are prevented by this measure.
   Depending on the share of OHL, MV networks either have RG or Low Ohmic Neutral Earthing (LONE). As with RG the earth fault current is minimized, continued operation is possible for single pole faults.
   Due to limitations concerning the network expansion, isolated neutral points are mainly used in either LV networks or industrial MV networks. During earth faults, the network operation is continued, granting high availability. Additionally, electric arcs are distinguished without further measures for the capacitive fault current is small enough.

4. Interferences
   As a side effect of the ultimate magnitude of the fault current (which is strongly influenced by the neutral point treatment), possible interferences have to be considered. High currents may induce voltages in telecommunication lines or other cable loops nearby, causing possibly dangerous potential

differences. Furthermore a major requirement for LONE, leading to high fault currents, is a sufficient grounding system. Ideally a global earthing system is given, providing a proper starting point for the following network design process regarding practical aspects (possibilities for earth fault protection schemes) as well as normative guidelines.

5. Earth potential rises - touch- and step-voltages

This actually is a further interference, as the ultimate impact on the resulting EPR as well as step- and touch voltages is given (aside from the share of the fault current given by the capacitive current provided by the sound network parts) by the grounding system. The earth return impedance $\underline{Z}_{ER}$ used in section 4, section 4.2.4 respectively, is a very useful, still massive simplification of the actual ohmic conditions. For the design process of earth fault protection schemes the use of $\underline{Z}_{ER}$ is adequate. If a change in neutral point treatment is pursued, a careful evaluation is necessary.

A thorough analysis of the grounding system is a time consuming and occasionally complex process, as network grounding systems are grown structures. A contribution to the evaluation of grounding systems is given in [24]. An intricate model of urban grounding structures is also presented in this work, leading to a more precise description of the earth impedance.

6. Availability - network reliability

In this thesis, the term availability is used for either equipment parts or certain points, e.g. Ring Main Unit(s) (RMU), within the network. Network reliability is described by IEEE indices and provides average *non-availabilities* for a defined section, network part or even the whole network. The definitions are given in section 3.1.1.

In section 2.2 a summary of equipment damage rates is given. Those quite clearly show the steep rise of damage rates of cable and cable accessory over the years. While the general ageing of network equipment cannot be entirely prevented, precautionary considerations could slow down the process. Austrian as well as German MV networks generally show high availability, leading to very low network reliability indices. This partly is achieved by the continued operation of resonant grounded networks during single pole faults. Nevertheless the availability of urban MV networks seems to decrease due to a higher rate of double earth faults, cross-country faults respectively. As restoration times are significantly higher for this type of fault, the advantages of continued operation become less important. Simultaneously the selective interruption of faulty branches gains relevance, as

by this means an elevation of the line-to-ground voltage is prevented, avoiding serious stress to equipment insulations and therefore possibly extending equipment life time. A selective interruption of faulty branches is easier to achieve in Low Ohmic Neutral Earthing cable networks. Thus the choice of neutral point treatment once more influences the earth fault treatment not only by means of choice of algorithm (see section 2.3.2) but also by allowing or even demanding a different type of operation.

### 2.3.2 Choice of Earth Fault Protection Scheme

The choice of earth fault protection is strongly influenced by both the type of network (neutral point treatment, share of cable, system length, network structure) as well as economic aspects which are mostly defined by life cycles of equipment parts, need of additional (measurement) devices etcetera.[5]

1. Neutral point treatment

   - In terms of earth fault protection, for the *isolated neutral point treatment*, the use of harmonics is one possible option. Depending on the degree of harmonic distortion, the measurement of the currents using natural harmonics might be enough. As this method is not as suitable for ring structures as it is for radial networks or open loop structures, the $sin(\varphi)$ method possibly is a better choice for urban MV networks.

   - Networks using *Resonant Grounding* could as well be equipped with earth fault detection using harmonic components. A further possible measure is the pulse method. Similar to the use of harmonic components without further decision criteria (such as the displacement voltage in the $sin(\varphi)$ method), the pulse method does not work for closed ring structures unless further measures are implemented (see section 4.2). Additionally, meshed network structures exclude the pulse method. Therefore, the active residual current method seems to be the best option for resonant grounded MV networks. Depending on the ohmic losses of the network, an increase of the active residual current using one of the methods described in section 4.2.4 can be reasonable.

   - *Solidly grounded networks* provide a very high earth fault current. Its magnitude reaches the amperage of short circuit currents. Therefore,

---

[5] The decision criteria given in the list is enumerated solely for structure purposes. There is no intention to prioritize the given aspects. Also this list is not exhaustive.

an implementation of additional earth fault detection is not necessary. As a consequence of the high fault current during single pole faults, the faulty branch is (must be) switched off. The faulty section is identified with over-current indicators. Depending on the network operation strategy an automatic re-closer might be implemented, to minimize non-availability in case of temporary faults.

2. Existing equipment - costs factors
   Some earth fault detection systems use equipment parts, which are already in use within the network. Therefore, the implementation of such an protection scheme may be less expensive than others (see section 4.2).

3. Fault current and admissible step- and touch voltage
   One way of choosing between the systems using a deliberately increased detection current (mostly by increase of the active residual current) is the choice by desired amperage of the detection current.
   The current may be limited by the admissible touch- and step voltage, which can be estimated as the product of the detection current and the so called earth return path impedance $Z_{ER}$.
   A further limitation could be caused by possible interferences (see section 2.3.1).
   If the increase of the active residual current method is considered, it can be distinguished by the resulting (or aspired) detection current:

   – 10 A : parallel resistance typically connected to auxiliary winding of the Petersen coil (classic approach). This method is restricted by the share of capacitive current, as the resulting angle between the displacement voltage and the active residual current is the critical variable.

   – 60 A : resistance directly parallel to Petersen coil (often referred to as watt-metric STLONE)

   – 300 A : resistance directly parallel to Petersen coil (often referred to as ampere-metric STLONE)

   – 1000 A : Ampere-metric STLONE
   Either long or short operation of the parallel resistance, depending on the operation mode (continued operation (short time high current injection through parallel resistance) vs. immediate tripping (long time high current injection).

   – HPE: around 1 kA

The decision criteria given in this list may seem sparse compared to the one for the choice of neutral point treatment (see section 2.3.1), many points could easily be swapped between those two enumerations though. Thus both should be considered during an earth fault protection design process.

# 3 Earth Fault Treatment as an Influence on Network Reliability

Due to previous work by the author, this section may resemble publications such as [**1**], [**2**], as well as [**25**].

## 3.1 Reliability Assessment

An impartial comparison of electric grids is, due to multiple impact factors on node voltages, losses and reliability, difficult to accomplish. As stated in [**2**] (author's contribution), the average system performance can be measured by duration and frequency of customer interruptions. Still an awareness of the characteristic of average values of reliability, which can only give general trends which entail a loss of detail, is assumed.

Concerning reliability assessment, there is a distinction between the deterministic approach (also known as (n-1)-criteria) and the probabilistic method. For this thesis, the probabilistic method was used to obtain reliability indices for an exemplary network.

### 3.1.1 Reliability Indices according to Institute of Electrical and Electronics Engineers (IEEE)

In this section, the calculation of reliability indices according to Institute of Electrical and Electronics Engineers (IEEE) [26] is explained. By the use of reliability values for each station in the medium-voltage network for the given equations, reliability indices can be obtained. The network calculation software NEPLAN® is used to calculate these reliability values.

**System Average Interruption Frequency Index (SAIFI)**

The index SAIFI according to Equation 6 gives the average interruption frequency of customers for a lasting interruption within a defined time range (usually one year).

$$SAIFI = \frac{\sum \text{Total Number of Customers Interrupted}}{\text{Total Number of Customers Served}} \tag{6}$$

**System Average Interruption Duration Index (SAIDI)**

The index according to Equation 7 gives the total time of interruption for the average customer during a defined time range. SAIDI is usually given in minutes

or hours per year.

$$SAIDI = \frac{\sum \text{Customer Minutes of Interruption}}{\text{Total Number of Customers Served}} \qquad (7)$$

**Customer Average Interruption Duration Index (CAIDI)**

The calculation of the average interruption time is described in Equation 8.

$$CAIDI = \frac{\sum \text{Customer Minutes of Interruption}}{\text{Total Number of Customers Interrupted}} \qquad (8)$$

**Average System Interruption Frequency Index (ASIFI)**

The calculation of ASIFI (Equation 9) is weighted by the load (in kVA) rather than the number of customers. This index is used for areas with few customers and high load densities [26]. A typical example is an industrial network. In Austria it is also the preferred index in terms of incentive based regulatory regimes (see section 6.4). In networks with evenly distributed loads, ASIFI converges towards SAIFI.

$$ASIFI = \frac{\sum \text{Total Connected kVA of Load Interrupted}}{\text{Total Connected kVA Served}} \qquad (9)$$

**Average System Interruption Duration Index (ASIDI)**

As well as ASIFI, ASIDI is weighted by the load, rather than the number of customers not supplied. This index is calculated according to Equation 10.

$$ASIDI = \frac{\sum \text{Connected kVA Duration of Load Interrupted}}{\text{Total Connected kVA Served}} \qquad (10)$$

### 3.1.2 Calculation of IEEE-Indices from NEPLAN$^{\textcircled{R}}$ Simulation Results

In this section, the assessment of customer- or load-weighted reliability indices according to IEEE by the use of NEPLAN$^{\textcircled{R}}$ simulation results is explained. This approach has been presented in [**2**].

In order to determine every possible interruption combination in NEPLAN$^{\textcircled{R}}$, each switching option has to be added to the network simulation model. [**2**]

The interruption duration and frequency for each grid element is a simulation result. They characterize the interruption behaviour of the specific network element. The statistical data of the »FNN-Interruption-Statistics« is used as standard global input data for NEPLAN$^{\textcircled{R}}$. Reliability values for each grid element

are computed and then used in calculating the reliability indices and evaluating average system performance.

In Equation 11 and Equation 12, the calculation of customer based reliability indices are given.

$$SAIDI = \frac{\sum Q_i \cdot K_i}{N_T} \tag{11}$$

$$SAIFI = \frac{\sum N_i}{N_T} \tag{12}$$

$Q_i$      Non-availability in $\frac{min}{yr}$

$K_i$      Number of customers per station

$N_i$      Interruption duration expected (T) multiplied by the number of customers per station ($K_i$)

$N_T$      Total number of customers in the network

The average required time for restoration of energy supply is calculated by using Equation 13.

$$CAIDI = \frac{\text{SAIDI}}{\text{SAIFI}} \tag{13}$$

The load-weighted indices ASIFI and ASIDI are calculated as stated in Equation 14 and Equation 15. [2]

$$ASIFI = \frac{\sum L_i}{L_T} \tag{14}$$

$$ASIDI = \frac{\sum Q_i \cdot S_i}{L_T} \tag{15}$$

$Q_i$      Non-availability in $\frac{min}{yr}$

$L_i$      Multiplication of expected interruption frequency (F) by transformer capacity of the station i ($S_i$)

$L_T$      Total transformer capacity of the network; sum of transformer capacities

## 3.2 Methodology - Probabilistic Method

The following chapter summarizes the general approach to answer the research questions given in section 1.6. Due to previous work, this section may resemble publications such as [1], [2], as well as [25].

In order to achieve simulation results as close to real networks as possible, a network model of an existing suburban area is being used for reliability calculations. In doing so, the results for a basic network configuration can be verified, providing an optimum starting point for the planned variations. The suburban cable network whose nominal voltage is 20-kV consists of:

- approximately 150 MV/LV transformers (20-kV/0,4-kV)

- approximately 80 system kilometers of cable lines

- 30 circuit breakers in RMU

- approximately 40 disconnectors

- capacitive current 150 A, 5 percent overcompensation

In its basic configuration, the network provides a resonant earthed neutral system. In a first draft, the network reliability is calculated for a number of interruption frequencies and interruption durations (see also Table 6).

After several variations to the original interruption statistics and reliability assessment, the probabilistic method of reliability assessment discussed in section 3.2.1 turned out to be the wrong method to show the actual influence of earth faults, cross-country faults respectively, on the overall network reliability.

Statistically, in resonant grounded MV networks, earth fault induced interruptions are not relevant. The main reason for this is the partly meshed network structure itself, which provides sufficient switching options, as well as the operation mode, characterised by remotely controlled CB in RMU. As a result, a single line-to-ground fault never leads to statistically relevant interruption durations in partly-meshed network structures.

As these insights followed a probabilistic approach to reliability assessment, the applied method is described in section 3.2.1 even though it did not provide the anticipated results. As a consequence, an analytic approach was followed.

ELECTRICAL
POWER SYSTEMS
TU GRAZ

### 3.2.1  Probabilistic Method - Reliability Assessment

For this method, all relevant interruption combinations (in terms of statistical interruption behaviour) are combined and analysed. By using especially prepared datatypes and the given switching options as well as switching times after an interruption, the reliability values for each grid element are computed. Therefore, all information needed for the assessment of reliability indices are gathered in this process. [27]

The exact procedure of the probabilistic method is described in Figure 9. A more detailed description of the overall process is given in [27], [**2**] or [**25**].
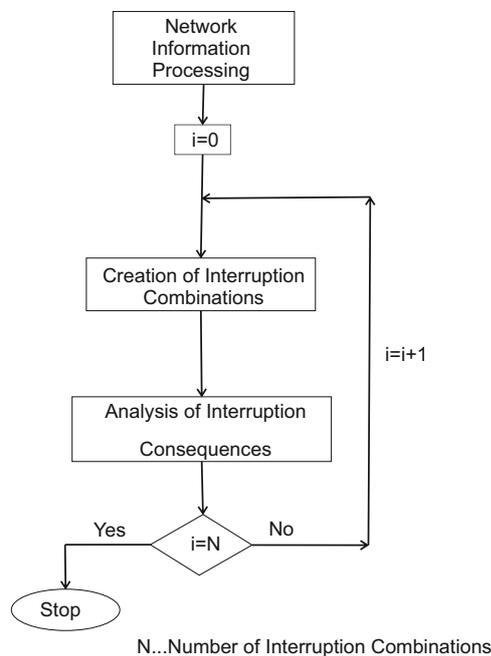


Figure 9: Probabilistic method of reliability assessment process chart, [27]

One advantage of the probabilistic method is the assessment of unreliability, giving the opportunity of customer related conclusions. This is achieved by rather elaborate modelling and computation. Despite the high level of automation, possible by using network calculation software, interpretation of the results remains an engineer's assignment, as suitable assessment criteria has to be defined. [28]

**Reliability Quantities**

By incorporating specific failure behaviour of network equipment, protection settings and switching times after an interruption, reliability indices can be calcu-

lated. The network calculation software NEPLAN$^{®}$ computes data (given in Table 6), referring to the stations of the given network; network nodes respectively. [27]

In the next step, the network reliability is assessed.

Table 6: Reliability quantities computed by NEPLAN$^{®}$, [27]

| Acronym | Reliability quantity | Unit |
|---------|---------------------|------|
| F | Expected value of the interruption frequency | 1/a |
| Q | Non-availability | min/yr or h/yr |
| T | Expected value of the interruption duration | min or h |

Finally the process of reliability indices assessment is summarized in Figure 10.
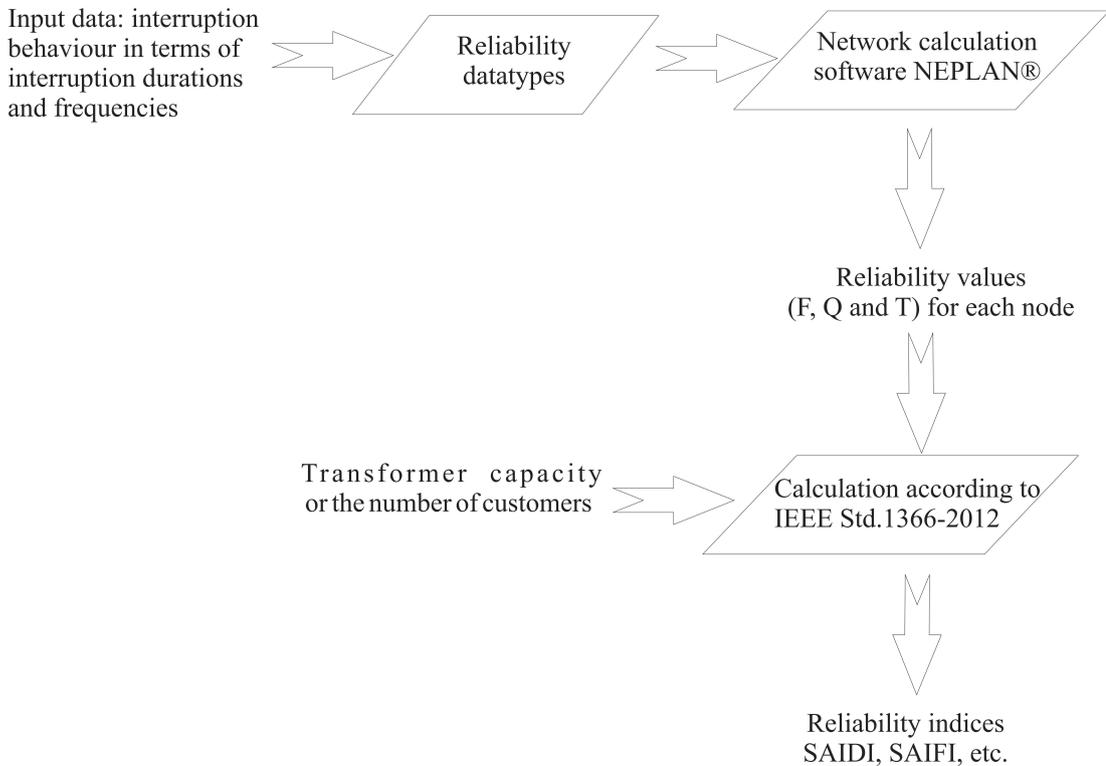


Figure 10: Process chart for calculating reliability indices, [**2**]

## 3.3 Analytic Evaluation of Non-Availability as a Consequence of Earth Faults

Due to the difficulty of validating the numerics of the probabilistic method, the impact of earth faults is analysed step by step for several fault locations and network structures. The network structures used for this sections are listed and discussed in [29]. The goal of this analysis is to find the most challenging combina-

tion of fault locations for single and double earth faults within electrical networks.

According to FNN fault statistics ([30]), around one third of single faults causing interruptions in energy supply are earth faults. The frequency of occurrences causing interruptions in MV networks was $\frac{2.34}{yr \cdot 100km}$ as a five-year-average. The frequency of earth faults in German MV networks was $\frac{0.77}{yr \cdot 100km}$ (for all types of neutral point treatment). In isolated and resonant grounded networks, the frequency of earth faults reaches a slightly higher value of $\frac{0.947}{yr \cdot 100km}$. There is also a remark on the frequency of multiple earth faults which necessitate manual switching actions in isolated networks or RG networks, which was $\frac{0.286}{yr \cdot 100km}$ in 2016.

### 3.3.1 Radial Network Type

In strictly radial networks, there are no connections between the MV branches of the grid. This means, there are no switching options allowing a supply by the means of another network branch. This type of network design is used for sparsely populated areas. In case of an interruption, there is apart from emergency generators no way of supplying customers downstream. As the probability of a fault rises with the system length, the non-availability for customers at the end of a network branch in radial networks is higher than for customers at the beginning. This network type is chosen for its simplicity in operation as well as protection. Usually a DMT protection scheme is sufficient. The current threshold for the DMT relay must not be higher than the lowest possible short circuit current in the given network. The lowest possible short circuit current is calculated by considering a line-to-line fault while taking into account the effects of electric arcs.
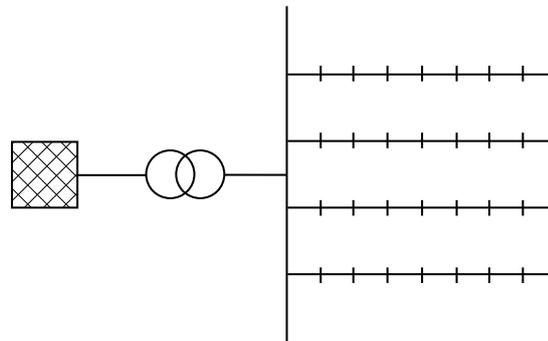


Figure 11: Schematic diagram of a radial network with four branches and seven stations (customers respectively) per branch

## Minimal Example

To give an impression on the relations, a simple example for the network shown in (Figure 11) is calculated. In order to assess the non-availability as a consequence of single earth faults for each customer station, the frequency of earth faults causing interruptions $H_{e/f} = 0.33 \cdot \dfrac{2.34}{yr \cdot 100km} = \dfrac{0.77}{yr \cdot 100km}$ is used, as the share of single earth faults in MV networks is one third of the single faults causing interruptions in energy supply. Even though operation is continued during earth faults, the affected network branch has to be interrupted.

If a distance between customer stations of 250 metres is assumed a frequency of interruptions for each station can be calculated. The frequency of interruptions can be written in vector form, while each vector represents one branch of the considered network.

In this example, the frequency of interruptions per branch of

$H_{j,e/f} = \begin{bmatrix} 0.00193 & 0.00386 & 0.00579 & 0.00772 & 0.00965 & 0.01158 & 0.01351 \end{bmatrix} \dfrac{1}{yr}$ is

calculated for the customer stations (index j indicates the branch, index i indicates the respective station of the branch).

The first element of the vector represents the frequency of the network branch's closest customer to the transformer station. The last element represents the interruption frequency of the farthest station within the radial network branch.

The non-availability is defined as the product of the interruption frequency and the interruption duration (see Equation 16).

$$Q = H \cdot t_{interr} \tag{16}$$

$Q$      Non-availability in $\frac{min}{yr}$

$H$      Interruption frequency in $\dfrac{1}{yr \cdot 100km}$

$t_{interr}$      Interruption duration

If an interruption duration of one hour is assumed, this interruption frequency entails according to Equation 16 a non-availability of

$Q_j = \begin{bmatrix} 0.11583 & 0.23166 & 0.34749 & 0.46332 & 0.57915 & 0.69498 & 0.81081 \end{bmatrix} \dfrac{min}{yr}$.

The non-availabilities of one network branch are shown in Figure 12.
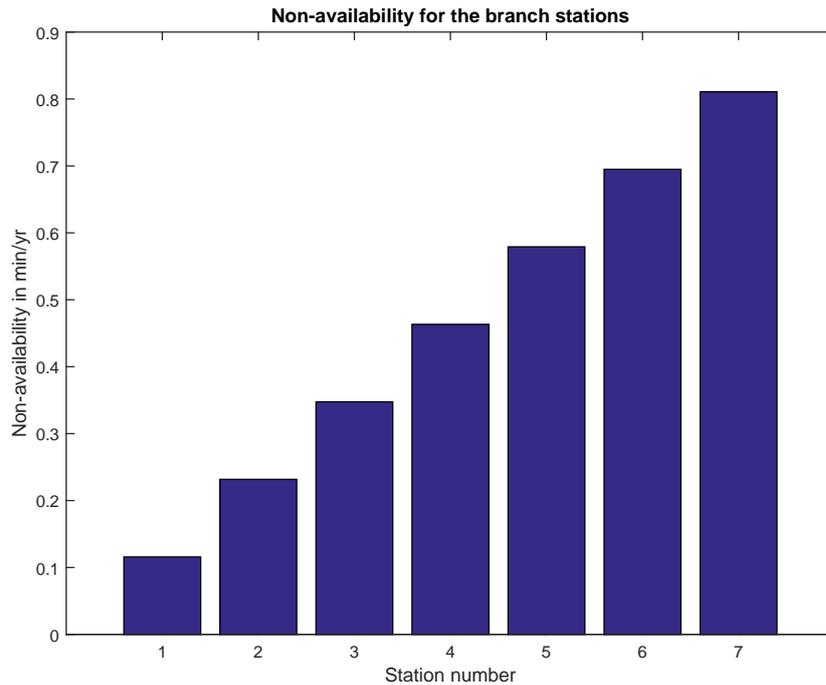
Figure 12: Statistic non-availabilities of network branch stations based on frequency of interruptions and system kilometre

The logic described above is applied to calculate the non-availability for every possible earth fault location in the network. The calculated non-availabilities are collected in a matrix of matrices, whereby each "sub-matrix" contains the non-availability resulting from a specific earth fault location (e.g. the earth fault is in section three of branch two would cause every station - beginning with station three - downstream to be interrupted for $t_{interr}$ ). Equation 17 represents the "sub-matrix", which includes the non-availability for each network station in case of the earth fault location given in Figure 13.



Figure 13: Earth fault in branch two, section three: all station downstream (pink area) are interrupted for $t_{interr}$

$$Q_{23} = \begin{bmatrix} 0 & 0 & 0 & 0 & 0 & 0 & 0 \\ 0 & 0 & 0.34749 & 0.34749 & 0.34749 & 0.34749 & 0.34749 \\ 0 & 0 & 0 & 0 & 0 & 0 & 0 \\ 0 & 0 & 0 & 0 & 0 & 0 & 0 \end{bmatrix} \frac{min}{yr} \qquad (17)$$

$$Q_{av.} = \frac{\sum Q_{ji}}{n} \qquad (18)$$

$Q_{av.}$      System average non-availability in $\frac{min}{yr}$

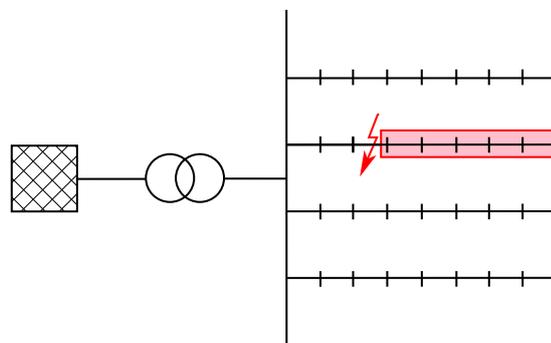$\sum Q_{ji}$      Sum of all non-availabilities caused by the earth fault locations considered for the example, j indicates the branch number, i indicates the station number

$n$      Number of non-availabilities obtained by considering every possible earth fault location within the network

The obtained matrix of non-availabilities derived from every possible earth fault location is used to calculate the average non-availability caused by earth faults for the given network. The system average non-availability of this example is calculated according to Equation 18 and reaches 0.05 minutes per year, three seconds per year respectively.

As for this minimal example the load of each customer station is assumed to be the same, the average non-availability is equal to ASIDI (see Equation 15 and the derivation given in Equation 19).

$$ASIDI = \frac{\sum Q_i \cdot S_i}{L_T} \overset{P_i = P_n \forall i}{=} \frac{S_n \cdot \sum Q_i}{N \cdot S_n} = \frac{\sum Q_i}{N} \qquad (19)$$

$Q_i$      Non-availability in $\frac{min}{yr}$

$S_i$      Transformer capacity of the respected station

$L_T$      Total transformer capacity of the network; sum of transformer capacities

$S_n$      Transformer capacity

$N$      Number of transformers (stations respectively)

**Earth Fault Treatment in Resonant Grounded Radial Networks**

As radial networks are typical for remote areas as well as sparsely populated areas, they are more likely to consist of OHL, than cables. Therefore, *resonant grounding* is a typical neutral point treatment. The advantages of RG such as continued

operation during earth faults, the distinguishing of transient earth faults, as well as the reduction of the earth fault current to a minimum (defined by the degree of detuning) work out well for this network type. As the structure is - per definition - not even partly meshed, each interruption leads to Energy Not Supplied (ENS) for each customer downstream. This effect is moderated by the continued operation during earth fault, as the stations are supplied until the faulty section has to be interrupted for repair measures. Nevertheless, for repair works interruptions have to be accepted. Double or multiple earth faults worsen the situation, as the interruption duration increases with each additional fault. Also ENS increases unless the second earth fault occurs downstream the first fault (this scenario only applies to RG).

Earth fault detection only by the means of DMT is not advisable for this type of neutral point treatment, as earth fault currents generally do not reach the level of threshold phase currents. STLONE potentially works, as the fault detection is automated and therefore works faster than the trial and error method.

Long distances between the busbar and possible fault location - which are likely in radial networks - have to be considered during the design process (see section 4.2.5).

Furthermore the interruption duration is not affected by the detection method, as it is defined by the time needed for repair measures. Therefore, for high interruption durations, the impact of a fast earth fault detection method is very limited. The same considerations apply to the HPE method. Additionally HPE is not as suitable for OHL-dominated networks, as for cable structures. Due to potentially high transfer impedances, the detection current in OHL networks is limited. The use of harmonics as in the $sin(\varphi)$-method can be implemented if the level of harmonic distortion is high enough and resonances are avoided. Therefore, the customer structure, the types of load within the network respectively, influence the suitability. The pulse method works out for radial network structures. For a low number of branches, this method might also be an economic choice, for earth fault detection purposes.

### 3.3.2 Open Loop Structures

Open loop structures ensure lower interruption durations, as a CB connect two radial branches with each other (see Figure 14). Therefore, by a simple (in best cases automated) switching operation, in case of interruption caused by a single fault, customers located downstream of the fault location but in a sound section of the branch can be supplied from the neighbouring branch. In order to achieve

this, the faulty section has to be disconnected first. Automated stations offer very low switching times, which increases the availability of a network. If there is no automated switching in the faulty branch, the affected section has to be disconnected by manual switching, which may take between fifteen minutes (in urban areas, where travelling times between stations are low) or around one hour (in rural areas with high travelling times).
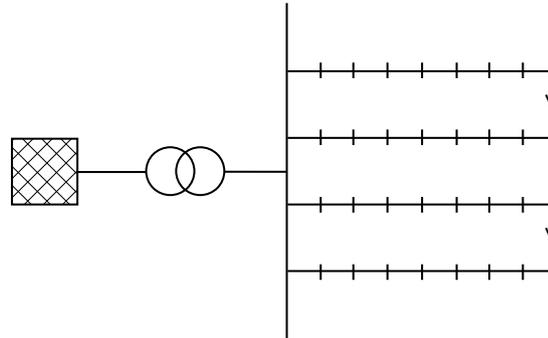


Figure 14: Schematic diagram of an open loop network structure

Only in the event of interruptions which overlap in time in both half-loops, the interruption durations increase by the percentage of overlap (see Figure 15). The maximum interruption duration reaches the restoration time (time needed for repair measures respectively). In such cases the resulting non-availability is equal to the one in an equivalent radial network. Because both half-loops hold reserves for possible interruptions in the neighbouring branch, network branches in open loop structures should not be loaded with their nominative load. The planning principles presented in [29] suggest a use to sixty percent of the nominative current. For the protection of the MV cables in open loop structures DMT is sufficient.

(a) Time Overlap 0 %

(b) Time Overlap 20 %

(c) Time Overlap 70 %
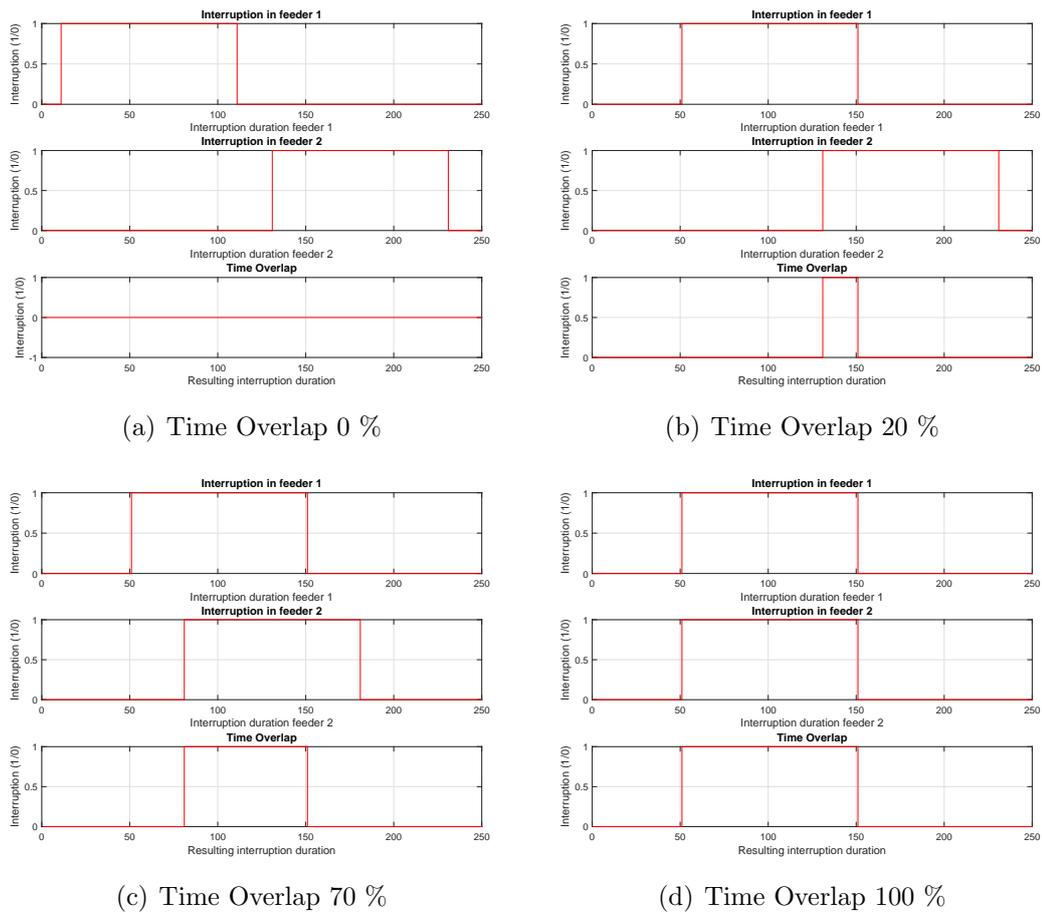
(d) Time Overlap 100 %

Figure 15: Consequences of time overlap of interruptions in both half-loops on total interruption duration for "healthy" network sections

**Earth Fault Treatment in Open Loop Structures**

In case of an earth fault in a resonant grounded MV network, the operation can be continued for some time. Still, for repair measures, there has to be an interruption for at least the faulty segment. The sound network parts are only affected for the time needed to restore supply via the CB connecting two half-loops with each other. As mentioned before, only the case of two time overlapping faults in the two half-loops of an open loop structure reaches interruption durations equal to the restoration time.

Earth fault detection schemes using the active residual current, such as STLONE and HPE, are suitable methods to decrease the time needed to find the faulty network section. As urban MV networks often are considered to provide a global earthing system, even high detection currents are acceptable. High detection currents are frequently required for the determination of the faulty section (versus determination of the faulty feeder - "standard earth fault detection") via overcurrent indicators.

Elisabeth Hufnagl

The adequacy of the network's earthing system has to be verified beforehand. If there is no way to prove the suitability of the earthing system, the implementation of a STLONE using a rather low detection current (watt-metric) is necessary. Additionally, the improvement of the grounding system is highly recommended. The use of harmonics for earth fault detection purposes is, as mentioned in section 3.3.1, limited to networks showing a sufficient degree of harmonic distortion. The pulse method relies on a sufficient deviation from the design residual current. To ensure the function of the pulse method in (open) loop structures, a work-around offered in section 4.2.2 can be applied.

The open loop structure is a common basis for urban electrical networks. Due problems with aged cable structures, continued operation during earth faults can develop into double or even multiple earth faults, confronting DSO with considerable efforts in restoration. While [30] does not distinguish between single and multiple earth faults, an earlier analysis indicated a total of 6204 stationary earth faults concerning cables for the years 2004-2011 for German 20-kV MV networks with resonant grounding [31]. Multiple earth faults reached a number of 2100 in the same period of time for the same equipment parts and network type (see Figure 16) [31].
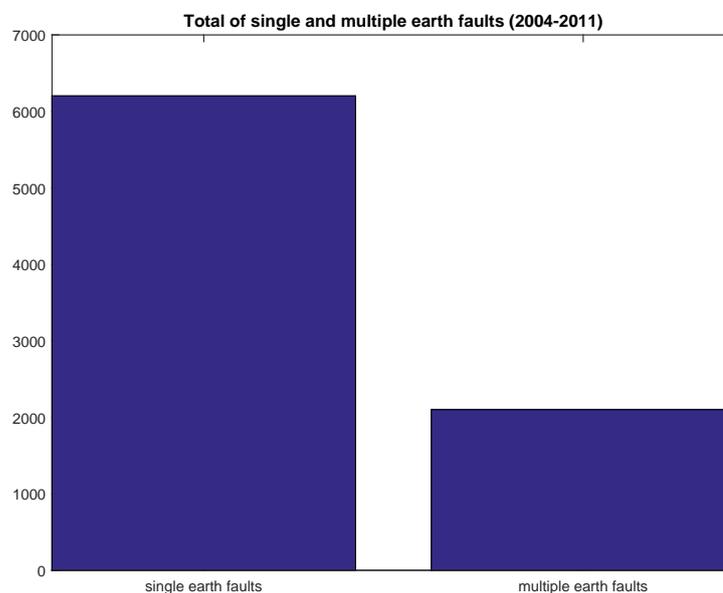


Figure 16: Total number of single and multiple earth faults in German MV cable networks operated with resonant grounding between 2004 and 2011 according to [31]

Several publications even imply, that fifty percent of stationary earth faults in urban resonant grounded MV networks develop into double or even multiple earth

faults.

A network showing a multiple earth fault rate as high as described above, which is also high in customer density (load density respectively) may benefit from a change in neutral point treatment. Even though the probability of a single earth fault may not be affected by the transition to LONE, the occurrence of multiple earth faults as a consequence of increased line-to-ground voltages is prevented, as stationary line-to-ground faults are not possible in LONE-networks. As earth fault currents reach the extent of short circuit currents, a protection scheme using DMT is sufficient.

## Minimal Example

For a better overview of the interruption duration to be expected in case of earth faults in LONE open loop structured urban networks, the following minimal example (similar to [5]) is given:

In one loop of the structure given in section 3.3.2 a high current earth fault occurs. The absolute earth fault current is designed to reach around 1 kA to trip DMT and overcurrent indicators. Therefore, it takes the delay time of the relay plus operating time of the CB to interrupt the fault current resulting into a total fault duration of $t_{e/f,duration}$.
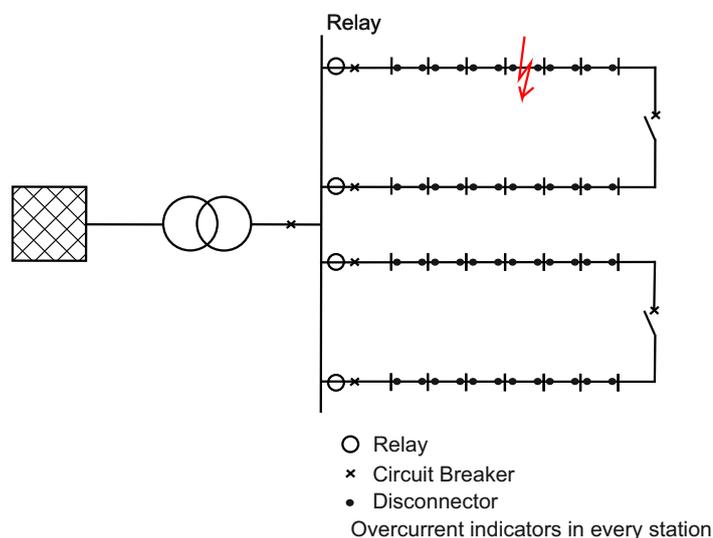


Figure 17: Open loop cable network (operated as LONE) minimal example for earth fault localisation process

Once the faulty branch is disconnected from the network, its stations are not supplied.

**Case 1**  If a dense distribution of three phase short circuit indicators connected to the control centre is assumed, the actual fault location can be narrowed down based on the indicators' reports. This should take just a few periods (e.g. $t_{indicators}$= 1 min). At this point, the disconnector (if available the remote controlled switch) closest to the fault location (but still upstream) is opened, followed by the closing of the CB of the branch. In doing so, all stations upstream the earth fault location are restored. If the earth fault affected section is known, the "healthy" sections downstream the fault locations can be restored by opening the first disconnector downstream the fault location and closing the coupling CB. Depending on the switching option (automated vs. manual) the time needed for this step varies between $t_{switching} = 5min$ (e.g. in Table 7) and hours (see $t_{travelling}$ in Table 7).

**Case 2**  If the short circuit indicators are not connected to the control centre, they have to be checked by a technician in order to determine the last indicator upstream the earth fault location entailing a significant travelling time. In urban areas an average travelling time of fifteen minutes between stations is assumed, still the time needed to reach the first station in the cause of earth fault localisation can take up to e.g. 90 minutes (large urban networks).
From here on, the actually faulty section is narrowed down by driving to the next short circuit indicator. The final step is the opening of the disconnector facing the earth fault downstream and opening the disconnector facing the earth fault upstream as well as closing the coupling CB of the half loop structure to restore all stations in the healthy sections of the branch.

Table 7 shows an exemplary timetable for the measures necessary in case of an earth fault between station number four and five (downstream).

Table 7: Exemplary timetable for earth fault treatment in LONE urban open loop structured MV networks

| Step in procedure | Duration | Example Values | Description |
|---|---|---|---|
| 1 | $t_{e/f,duration}$ | 0.5 sec | Time until the earth fault is interrupted |
| 2 | $+t_{indicators}$ | 1 min | Time needed to interpret information from short circuit indicators |
| 3 | $+t_{rest,upstr}$ | 5 sec - 90 min | Restoration time upstream stations; mainly depending on the type of switch: disconnector operated by manual switching (entails travelling time to the station) vs. remote controlled CB; by this time ($t_{e/f,duration} + t_{indicators} + t_{rest,upstr}$) three out of seven stations are restored |
| 4 | $+t_{travelling}$ | 10 min - 15 min | Travelling time needed to reach next station of the faulty branch |
| 5 | $+t_{switching}$ | 5 min | Time needed to interpret information from short circuit indicators and switching operation |
| : | : | : | : |
|  | $t_{total}$ | e.g. 100 min | **Total duration of restoration procedure** |

### 3.3.3 Closed Loop Structures

This type of structure is challenging in terms of protection schemes. Directional comparison protection is, as a consequence of the bidirectional supply, necessary for a secure and selective tripping of faults. For fault localisation purposes, distance protection is suitable. Due to the high effort and complexity, this network structure is not common.

### 3.3.4 Triple Network Structures

If operated with normally open switching positions, this structure does not differ from the radial or the open loop structure. There is no significant advantage of triple network structures in comparison to open loop structures except for selected outage scenarios. In those rare cases a restoration via the third branch is possible for parts of the other two branches. [29]
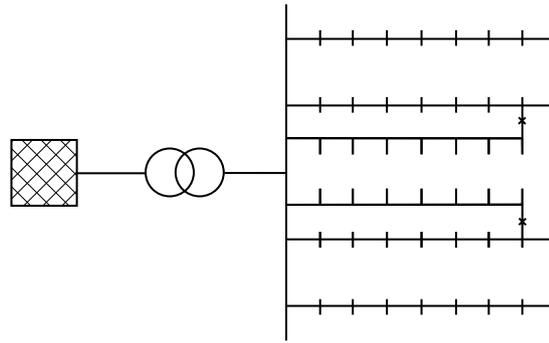
Figure 18: Schematic diagram of a triple network structure (x...CB positions)

### 3.3.5 Quadruple Network Structures

To give a more complete overview, the quadruple network structure is shown in Figure 19. Similar to the triple network structure, operated with normally open circuit breakers, there is no significant difference to the open loop structure except for selected outage scenarios.
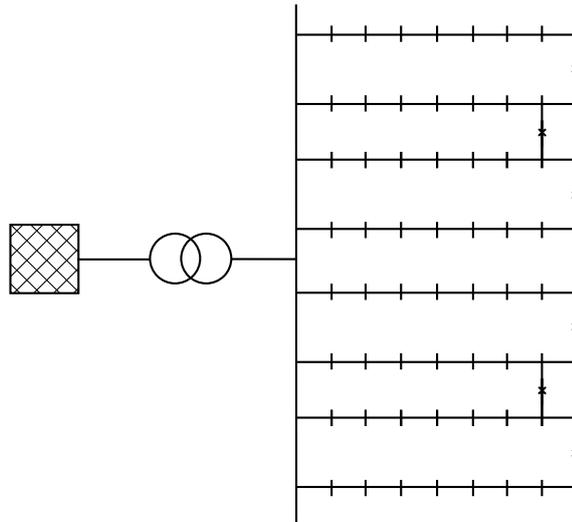


Figure 19: Schematic diagram of a triple network structure (x...CB positions)

# 4 Design of Earth Fault detection methods and their Cost Factors

Earth fault compensation enables the continued operation of a network during earth faults, which ensures a high reliability concerning short interruption durations. Nevertheless, distribution system operators of aged cable networks are questioning the practicality of this neutral point treatment, as risen phase to earth voltages due to earth faults cause major distress to aged insulation of cables and joints - which can cause further earth faults. As a result, cross country faults can occur, causing high fault currents and a more complex setting for earth fault detection.

This raises the question, if the continued operation during earth faults really is the most suitable scenario for every type of network. Depending on possible changes to the network, a re-evaluation of the network reliability as well as personal safety aspects have to be anticipated. The actual impact of a measure on the overall reliability (which depends on the customer structure and the network structure) should be analysed beforehand.

## 4.1 Fault Clearance Time and Restoration Time

Depending on protection scheme, topology and type of fault, the fault clearance time is well defined. It depends on the earth fault treatment, as earth fault detection takes a few seconds to work at most.

However, restoration time is especially influenced by the fault clearance time. Compared to manual operation the use of automated schemes (automated stations) can improve restoration times significantly - given the fault localisation applied enables in-depth localisation[6]. Using strategies discussed in [15] an optimized placement of distribution automation (automated schemes respectively) can be achieved. Considering an introduction of penalty payments, fast restoration and investments securing the former are essential.

## 4.2 Earth Fault Localisation Methods - Design and Cost Factors

In this section, various earth fault localisation methods as well as in-depth localisation methods are described. Cost factors relevant for economic analyses are

---

[6]In this thesis the term "in-depth localisation" is used for earth fault localisation methods enabling the determination of the affected branch section. Switching options by the means of disconnectors on both ends of a section are assumed

specified as published in [**4**] (author's contribution).

### 4.2.1 Earth Fault Detection Using Harmonic Components

Both methods described in this subsection basically use currents (their magnitudes) or angles for the determination of the faulty branch.

**Natural Harmonics Method**
Using the natural harmonics for earth fault localisation actually means the use of the 5th harmonic, as it usually is the strongest harmonic in the network. There are three procedures being used in earth fault detection relays:

- measurement of the 250-Hz-current.

- $\sin(\varphi)$ procedure

- comparing procedure

The first procedure simply demands relays in every branch. The significant property is the 250-Hz-current. As the Petersen coil (arc-suppression coil) represents a high impedance for 250-Hz-currents, the higher order harmonic currents return via the line-to-ground capacitances. Unfortunately, it does not work for ring structures or with high contact resistances. [9]
The $\sin(\varphi)$ procedure records the displacement voltage and the earth fault current. The significant property with this procedure is the angle between those two. In addition to the current measurement, a voltage transformer is necessary. [9][32]
If the 250-Hz-components of the branch currents are compared to each other, according to [33], the faulty branch can be distinguished from the solid ones using harmonic components as the significant property.

Regardless which of these three procedures is chosen, the harmonic distortion of the network may not be strong enough. The harmonic distortion shows a daily as well as a weekly profile. Therefore, technical requirements have to be verified before the implementation of one of these procedures.

The cost factors of this method are, [32]:

- earth fault detection relay capable of using harmonics

- summation current transformer (if $\sin(\varphi)$ procedure is used a voltage transformer)

**Forced Harmonics Method**

Earth fault detection using natural harmonics is not suitable for networks with low harmonic distortion. If an audio frequency remote control is already installed, an injection of a well defined signal for earth fault detection purposes is a possible solution.

Cost factors for this method, provided a radio frequency remote control is already part of the network, are

- suitable earth fault detection relay
- summation current transformer

### 4.2.2 Pulse Method

By temporarily connecting a capacitor parallel to the auxiliary winding of the transformer a detectable detuning of the earth fault compensation can be achieved. Considering high ohmic earth resistances, the pulsing has to be asymmetric. The overcompensation should in any case exceed the pulse current. [9]

In order to determine the faulty feeder, a suitable relay in every feeder is needed. The pulse method is not suitable for closed loop structures as well as meshed network structures unless additional measures are taken, to provide a work-around described below. The equipment parts needed for the standard pulse method depend on the mounting position of the pulse capacitor.

**Pulse Method in Closed Loop Structures**

In closed loop structures, the earth fault current flows in both half loops which can cause difficulties in detecting the injected pulse pattern as well as in determining the affected half loop. [9]

One work-around to this can be achieved by connecting the secondary sides of the respective current transformers of the half loops. By adding up the signals, the pulse pattern becomes more distinct. [34]

If an earth fault occurs in a closed loop structure, the earth fault detection relays in each half loop detect the fault. For a clear determination of the affected branch, the coupling CB is opened. Then the classic approach of switching off single feeders until the earth fault disappears is pursued. As the affected loop is already determined at this point, the switching effort and therefore the time needed for the faulty feeder determination is minimized. [34]

### 4.2.3 Active Residual Current Method

Due to zero sequence ohmic losses of the Petersen coil, overhead lines and cables as well as transformers, there remains a measurable active residual current, even if the earth fault is compensated. Using this method, the displacement voltage and the active residual current are measured and processed. To do so, a high accuracy of the angle for the measurement of the active residual current is necessary, as it is rather small. Therefore, suitable current transformers have to be chosen.

This method's cost factors are:

- earth fault detection relay capable of this method

- suitable current transformer

- suitable voltage transformer for the measurement of the displacement voltage

- engineering

### 4.2.4 Increase of Active Residual Current Method

An intentional increase of the active residual current can make its measurement and the determination of the angle between it and the displacement voltage less difficult. The active component of the residual current during earth fault compensation is considerably increased by e.g. connecting a resistance parallel to the auxiliary winding of the Petersen coil. Depending on the planned magnitude of the active residual current and the given opportunities in the network, various measures can be taken to increase the current.

**Parallel Resistance connected to Petersen Coil**
By connecting a resistance parallel to the auxiliary winding of the Petersen coil, the active residual current is increased. The magnitude of the current flowing through this circuit is limited due to the maximum load of the winding. This method is usually applied up to 10 A. If the capacitive component of the currents is too high, another method has to be applied, as no sufficient displacement can be accomplished.[35]
In order to use this method, the following equipment parts are necessary:

- earth fault detection relay capable of $\cos(\varphi)$ procedure

- power resistor

- low voltage contactor

- switching logic

- engineering

**Watt-metric Short Time Low Ohmic Neutral Earthing Method**
In connecting a medium to high ohmic resistance parallel to the Petersen coil (directly; no auxiliary winding used), the watt-metric STLONE is established. By this, the active residual current is increased up to 60 A.
This method's cost factors are:

- power resistor

- circuit breaker

- medium voltage cable

- switching logic

- earth fault detection relay capable of $\cos(\varphi)$ procedure

- engineering

**Ampere-metric Short Time Low Ohmic Neutral Earthing Method**
This procedure basically works the same as watt-metric STLONE, except the achieved current reaches up to 300 A, which enables an evaluation only taking into account the summation current. While a planned current of 300 A requires a summation current transformer capable of handling over-currents and a suitable earth fault detection relay, a intended current of 1000 A is detected by short circuit protection and over-current indicators (both equipment parts are often already in use in the network, which is why they don't have to be purchased for the sole purpose of earth fault localisation).
If the high current procedure (1 kA) is chosen, it has to be ensured that the step- and touch-voltages don't harm the boundaries given in [36]. Depending on the DSO's philosophy, a short operation of ampere-metric STLONE is used for the continued operation of the network during earth faults, or a long operation of ampere-metric STLONE is used for immediate tripping. The latter is, similar to the HPE method, limited to a certain amount of time, as high active power losses in the resistor can cause thermic stress and therefore possible damage.

**Healthy Phase Earthing Method**
The method of HPE equals a deliberately caused double earth fault [37]. Currents caused by this method range around 1 kA and flow for about 1.5 seconds

(orientation values), which means considerable thermic stress to the resistor. In order to avoid thermic damage to the resistor, a reasonable lag time is necessary before the procedure can be repeated. During the whole process, the neutral point treatment remains unchanged. Due to the high currents, there are no additional means of earth fault detection (determination of the faulty section) necessary, as the faulty feeder can be identified by over-current indicators. The actual fault location can be narrowed down, using short circuit indicators or even distance protection devices.

Cost factors with this method are [32]:

- medium voltage feeder and circuit breaker in transformer station

- two single phase circuit breakers

- power resistor

- control unit

- structural measures as e.g. foundation

- medium voltage cable

- engineering

Usually the equipment used for this detection procedure is already in use within the network.

It is clear, that the power resistor for the HPE method is a significant part of the equipment. The first step in the design process is the definition of the necessary current ($I_F$), attained by the HPE method. As a failure to operate of protection has to be avoided, the desired current should reach around a 50 % higher value, than the over-current indicator's activation current. As the fault loop impedance reduces the current, it's best practice to implement a factor of two (100 %) to ensure the function of protection devices even in the longest feeder. For a first approximation, the resistance of the HPE resistor can easily be calculated by Equation 20.

$$R_{HPE} = \frac{V_{ij}}{I_F} \tag{20}$$

$R_{HPE}$     resistor for HPE method

$V_{ij}$       line-to-line voltage

$I_F$       desired current for HPE method

Now $R_{HPE}$ can be used to calculate the actual current $I_{F,loop}$ using Equation 21.

$$\underline{I}_{F,loop} = \frac{\underline{V}_{ij}}{2 \cdot \underline{Z}_T + \underline{Z}_L \cdot (1 + \underline{k}_L) + R_F + R_{HPE}} \tag{21}$$

$I_{F,loop}$     achieved failure current in fault loop for HPE method

$V_{ij}$     line-to-line voltage

$\underline{Z}_T$     transformer impedance

$\underline{Z}_L$     line impedance, $\underline{Z}_L = z' \cdot l$

$\underline{k}_L$     earth impedance matching factor

$Z_F$     fault impedance (typically ohmic, e.g. arc resistance, therefore not in complex form)

$R_{HPE}$     resistor for HPE method

The earth impedance matching factor $\underline{k}_L$ is calculated by Equation 22.

$$\underline{k}_L = \frac{\underline{Z}_{ER}}{\underline{Z}_L} \tag{22}$$

$\underline{k}_L$     earth impedance matching factor $k_L$ (frequently used for distance relays)

$\underline{Z}_{ER}$     earth return path impedance

$\underline{Z}_L$     line impedance (positive sequence impedance)

The earth impedance matching factor $k_L$ used in this process is not to be confused with the k-factor $k_0$, which is given in Equation 23. Both of them are used in protection engineering for the distance relay, when it is used for earth fault detection respectively the calculation of the distance to the fault location.

$$\underline{k}_0 = \frac{1}{3} \left( \frac{\underline{Z}_0}{\underline{Z}_1} - 1 \right) \tag{23}$$

$\underline{k}_0$     k-factor $k_0$, "earth fault factor"

$\underline{Z}_0$     zero sequence impedance

$\underline{Z}_1$     positive sequence impedance

For a better understanding of the equation above (Equation 21), a closer look on Figure 20 can be helpful.
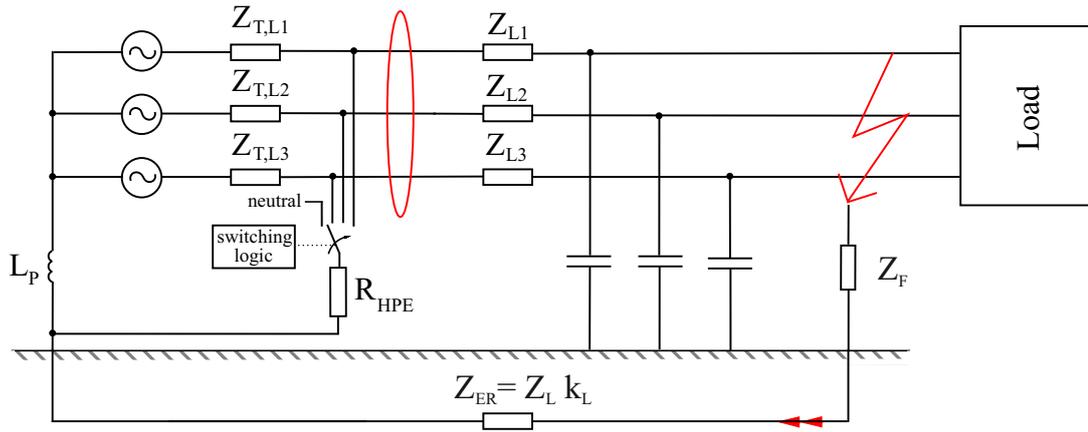
Figure 20: Earth fault detection the HPE method, [37]

The impedance $Z_{ER}$ does not actually represent the complete earth impedance but an approximation of it, which is based on some simplifying assumptions:

- A rather complex earthing system is reduced to a single impedance between the fault impedance $Z_F$ and the reference earth. A more detailed approach to the calculation of earthing systems and the fault current dispersion is given in [24].

- For the approximation of $Z_{ER}$ the earth impedance matching factor $k_L$ is used. This factor is usually used in distance relays. A sophistication of the earth fault detection and localization logarithm was proposed in [8].

The positive sequence impedance as well as the zero sequence impedance can be derived from the self-impedance and the mutual impedance. Their relation is described in Equation 24 and Equation 25.

$$\underline{Z}_1 = \underline{Z}_s - \underline{Z}_m \tag{24}$$

$$\underline{Z}_0 = \underline{Z}_s + 2 \cdot \underline{Z}_m \tag{25}$$

$\underline{Z}_1$      positive sequence impedance

$\underline{Z}_0$      zero sequence impedance

$\underline{Z}_s$      self-impedance

$\underline{Z}_m$      mutual impedance

The relations given in Equation 24 and Equation 25 can easily be derived by taking the steps given in section 8.1 (appendix).

The resistor $R_{HPE}$ is used for less than one to three seconds only. Afterwards the switching logic is locked for a lag time (in [37] a full hour is suggested), to make sure there's no further use of the automation until the resistor is significantly cooled. If the earth fault detection using HPE fails at the first try, for long lag times, there is basically no further use of it, as the classic approach (switching off single feeders until the earth fault disappears) would not take longer than waiting for the next try with HPE.

As one consequence it appears sensible, to calculate the actual thermic stress to the resistor, in order to reduce the cooling time. A detailed assessment of the thermic stress to the HPE resistor, as well as a calculation of the required cooling time is given in the following section.

If the HPE method is used for overhead line networks, one has to keep in mind, that due to longer distances and bigger fault resistances ($R_F$), the method becomes less suitable. As transfer resistances tend to be very small in cable networks, HPE works best with them.

### 4.2.5 Limits of the Active Residual Current Method

The following remarks concern analytic calculations using symmetrical components. The concept of symmetrical components was published in [38] in 1918 by C.L. Fortescue. In this thesis an introduction to symmetrical components is omitted.

Generally, there are some limitations that have to be kept in mind for the active residual current method. As a first step of the design process, the positive and the negative sequence impedances of the symmetrical components are calculated (see example in Figure 21).

$Z_1$ positive sequence impedance
$Z_2$ negative sequence impedance
$Z_{F,0}$ zero sequence impedance of the fault impedance
$Z_{ntr,0}$ zero sequence impedance of the system neutral
$Z_{L,0}$ zero sequence impedance of the line

$Z_N$ network (grid) impedance
$Z_T$ transformer impedance
$Z_L$ line impedance
$Z_F$ fault impedance
$Z_{ntr}$ neutral system impedance
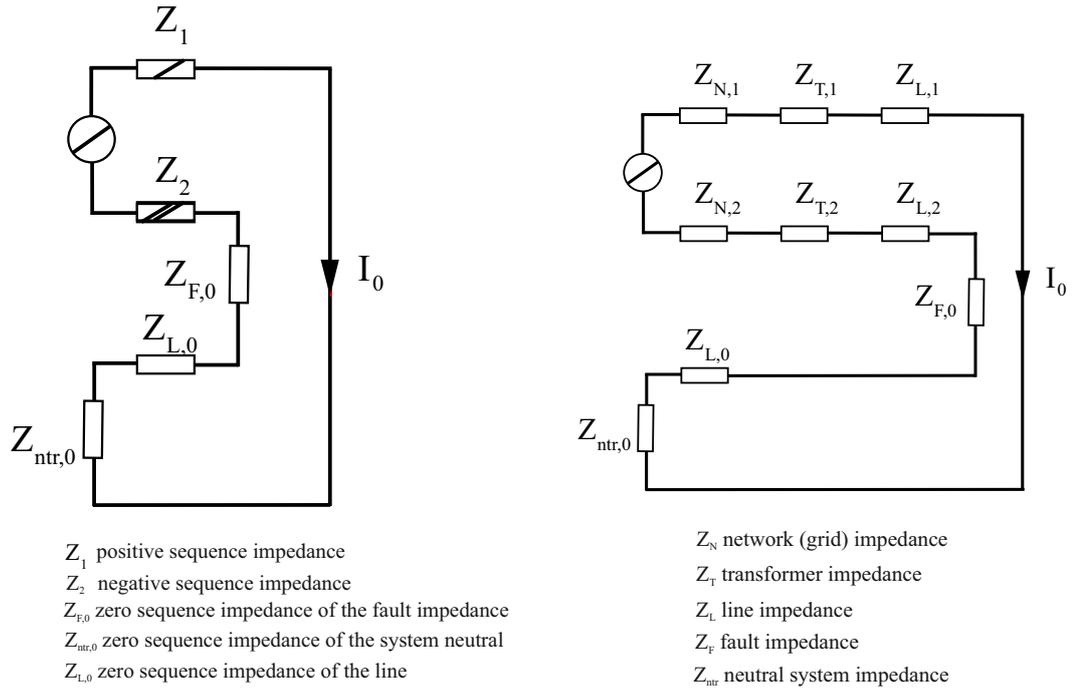
(a) Standard equivalent circuit for symmetrical components

(b) Example network in symmetrical components for the calculation of the zero sequence current

Figure 21: Equivalent circuits for the design process in symmetrical components

Then the capacitive reactance, as well as the parallel circuit in the zero sequence system is assessed. Taking the fault impedance into account, the total impedance can be calculated.

The resulting total current is the quotient of the line-to-ground voltage and the total impedance in symmetric components as stated in Equation 26. In case of a resonant or isolated neutral point treatment, the zero sequence system massively dominates the total impedance of the network in symmetric components for the fundamental frequency.

As stated in [3], the analytic calculation can be simplified, by focusing on the zero sequence system. In doing so, it becomes obvious, that the main influence on the total current is given by the transformer itself and its neutral point treatment. A high focus lies on the vector group of the transformer, as the current dispersion during faults and therefore the magnetic flux and its possible paths within the transformer define the magnetic impedance, which impacts the transformer's zero sequence impedance the most. This is why the active residual current method is not suitable for the Yy vector group, as its zero sequence impedance is too high to allow a detectable active residual current.

The reactive residual current is expected to be inductive, as resonant grounded networks usually are operated detuned to a certain percentage to achieve over-

compensation (see section 1.5). The active residual current mainly depends on ohmic losses of the transformer, the OHL (cables respectively), the Petersen coil and other network parts.

$$\underline{I}_{0,total} = 3 \cdot \frac{\underline{V}_{L-E}}{\underline{Z}_{total}} = \Re \left\{ 3 \cdot \frac{\underline{V}_{L-E}}{\underline{Z}_{total}} \right\} + \imath \cdot \Im \left\{ 3 \cdot \frac{\underline{V}_{L-E}}{\underline{Z}_{total}} \right\} \tag{26}$$

$\underline{I}_{0,total}$      total current flowing into the zero sequence system

$\underline{V}_{L-E}$      line-to-earth voltage (line-to-ground respectively)

$\underline{Z}_{total}$      total impedance in symmetric components

The reactive residual current, given in Equation 26 is the sum of the inductive current, which depends on the Petersen coil, and the capacitive current, which is defined by the network.

The main criterion when using the active residual current method is the angle between the displacement voltage and the total current at the relay location. This angle can be calculated, using Equation 27.

$$\varphi = 90° - \arctan \left( \frac{\Re \left\{ 3 \cdot \frac{\underline{V}_{L-E}}{\underline{Z}_{total}} \right\}}{\Im \left\{ 3 \cdot \frac{\underline{V}_{L-E}}{\underline{Z}_{total}} \right\}} \right) \tag{27}$$

As there are certain tolerances to current and voltage transformers, uncertainties to the measured angle have to be considered. Furthermore, the capacity of the faulty line itself has a worsening effect on the measured angle, as it influences the magnitude of the reactive residual current. The impact increases with the total distance between the busbar and the fault location.

Due to these uncertainties, an increase of the active residual current is sensible. As mentioned in section 4.2.4, the increase is achieved by either connecting a resistor to the auxiliary winding of the Petersen coil, or by connecting it directly parallel to the coil. Of course there is a difference in nominative current and therefore in active power losses, which has to be considered during the design process. The active residual current is increased by the value of $\frac{V_{L-E}}{R_{STLONE}}$.

Depending on the required angle (which is given by the used equipment and a security factor, e.g. 2) the active residual current can be calculated as stated in Equation 28. To make sure the method works even in the worst case scenario, the longest possible distance to the earth fault should be used for the calculation

of $I_{RR}$.

$$I_{AR,design} = I_{RR} \cdot \tan \varphi \tag{28}$$

$$I_{RR} = \Im \left\{ 3 \cdot \frac{V_{L-E}}{\underline{Z}_{total}} \right\} \tag{29}$$

$I_{AR,design}$    obtained active residual current

$I_{RR}$       reactive residual current

$\varphi$       angle between displacement voltage and total current in symmetric components

Finally, by using $I_{AR,design}$, the necessary resistor can be calculated.

**Sensitivity Analysis**

As mentioned before, the active residual current method in general, as well as methods relying on the increase of the active residual current, is sensitive to the system length and the fault resistance. In order to evaluate the impact of those properties, a sensitivity analysis for the zero sequence current was carried out (see Figure 22).
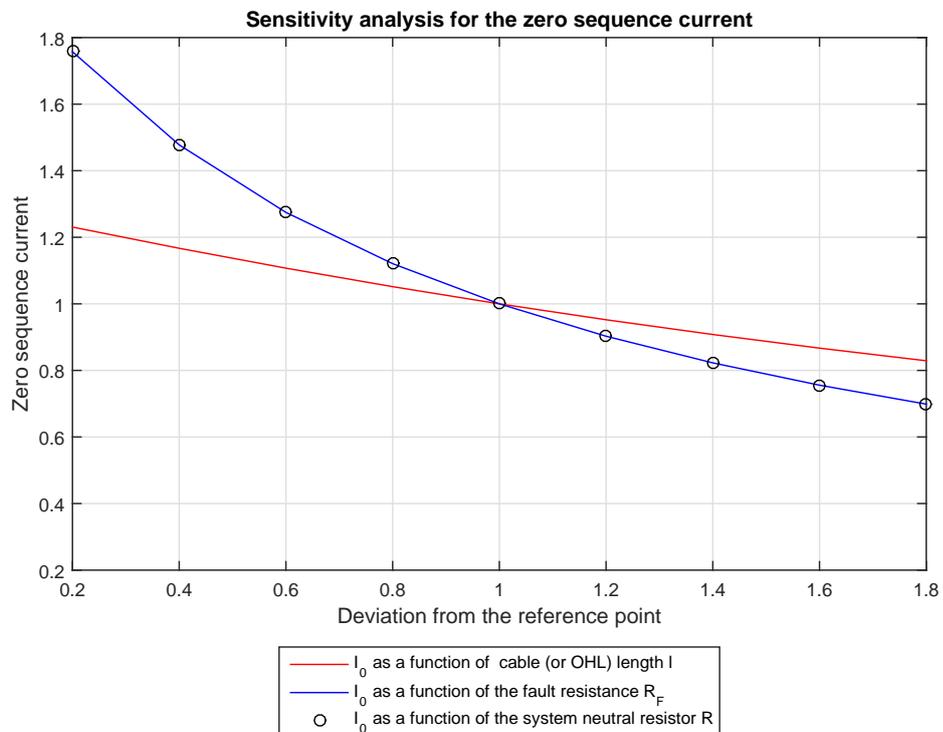


Figure 22: Sensitivity analysis for the zero sequence current in active residual current methods

Elisabeth Hufnagl

In Figure 22, the impact of the cable (OHL respectively) length, as well as the impact of the system neutral resistor on the zero sequence current and therefore on the fault current are shown.

Both the influence of the cable length, as well as the influence of the resistances in the zero sequence system show a non-linear impact on the zero sequence current (as can be expected regarding the calculation). The resistance in the zero sequence system shows a significantly higher impact on the resulting current than the cable length.

# 5 Thermic Stress to the Resistor used for High Detection Current Methods

High detection currents, as used in the ampere-metric Short Time Low Ohmic Neutral Earthing, for Low Ohmic Neutral Earthing or the Healthy Phase Earthing method, can cause considerable thermic stress to the system neutral resistor. As part of the design process of the earth fault detection method, the heating and cooling behaviour of the resistor should be evaluated. This chapter includes three successive models for an engineering approach to the assessment of thermic stress.

This chapter shows examples of the mechanic construction of power resistors (section 5.1) by the means of pictures taken in substations, as well as summarises the theoretical background of heat flow calculations (see section 5.2.2). Finally in section 5.2.3, with the help of simplifying assumptions, the qualitative thermic stress to a HPE resistor is assessed.

## 5.1 Mechanic Construction of Power Resistors

Most power resistors for protection purposes are mounted in a housing. The resistor itself takes only a small part of the housing's volume. The resistor basically can be considered as plates, arranged parallel to each other, as can be seen in Figure 23.



(a) Example for a STLONE resistor          (b) Example for a LONE resistor

Figure 23: Examples for system neutral resistances

Figure 24: HPE resistor (right hand side) and switching logic (on the left) as published in [37]

## 5.2 Analytic Assessment of Thermic Stress

The assessment of thermic stress to equipment parts is, especially in the case of free convection, a very challenging task. It frequently is a matter of concern to protection engineers, nevertheless it is not considered a field of expertise for electrical engineers in general. Still, under exceeding simplifying assumptions, some analytic calculations are achievable.

### 5.2.1 Methodology

For the the following engineering approach, the system neutral resistance is assumed to consist of parallel plates. The total volume of this arrangement of parallel plates is used for the calculation of an equivalent cube. Therefore, the resistor shows the same heating behaviour as a solid cube (enclosure neglected). The main task is the calculation of the cooling behaviour due to free convection. In the following three cooling models used in this assessment approach are compared to each other.

**Model 1**
The cooling behaviour of the system neutral resistor is calculated for a solid cube detached from its surroundings. For this first approach to the assessment of the cooling behaviour the thermal constants are expected to be exceedingly high, as the surface available for free convection is very limited.

**Model 2**
To take the actual surface of the assumed resistor into account, the solid cube of

*Model 1* is divided into the number of parallel plates assumed in the first place. The heat built up between the plates is neglected. For this model, the Nusselt Number and the significant length of the equivalent cube are used. Therefore, the heat transfer coefficient $\alpha$ obtained for *Model 2* is not accurate.

### Model 3

In order to assess the cooling behaviour of the arrangement of parallel plates as accurate as possible, it is assumed to be equivalent to a single vertical plate, if the same surface as in *Model 2* is assumed.
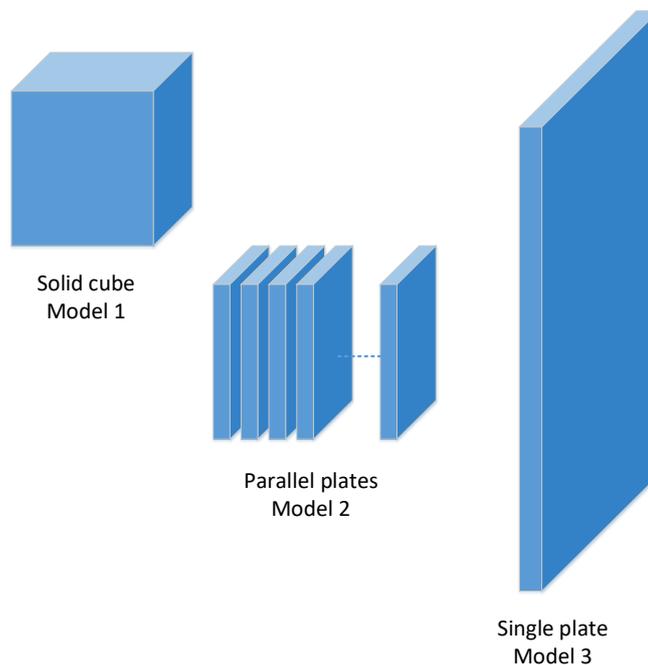


Solid cube
Model 1

Parallel plates
Model 2

Single plate
Model 3

Figure 25: Models to obtain heating and cooling behaviour of system neutral resistors

### 5.2.2 Theoretical Background

The physical relationships used for this section are a summary of the essential findings from [39] and [40]. Whereas for a very applications oriented approach the former is more helpful.

The first fundamental theorem of thermodynamics is given in Equation 30, [39]:

$$\Delta E = W + Q + E_M \tag{30}$$

$\Delta E$     change of energy within a system enclosed by its system boundaries

$W$     work

$Q$     heat which is transported solely due to temperature difference

$E_M$        energy transported by mass

A change of energy $\Delta E$ can only be achieved by a transport of energy, heat respectively, which exceeds the system boundaries. There are three types of heat transfer, [39]:

1. Thermal (heat respectively) conduction

2. Convection

3. Thermal radiation

The heat flow $\dot{Q}$ is defined as stated in Equation 31.

$$\dot{Q} = \frac{dQ}{dt} \tag{31}$$

$\dot{Q}$        heat flow, $[\dot{Q}] = 1$ W

$Q$        heat, $[Q] = 1$ J

$t$        time, $[t] = 1$ s

**The thermal conduction** mainly depends on the thermal conductivity $\lambda$. The formula for the heat flow density due to thermal conduction is given in Equation 32.

$$\dot{q} = -\lambda \cdot \frac{\partial T}{\partial x} \tag{32}$$

$\dot{q}$        heat flow density (general definition: $\dot{q} = \dfrac{d\dot{Q}}{dA}$), $[\dot{q}] = 1 \dfrac{W}{m^2}$

$\lambda$        thermal conductivity, $[\lambda] = 1 \dfrac{W}{Km}$

$T$        temperature, $[T] = 1$ K

$x$        length, $[x] = 1$ m

**The thermal convection** is obtained by assessing the heat transfer coefficient $\alpha$ first. The heat flow $\dot{Q}$ is calculated according to Equation 33.

$$\dot{Q} = \alpha \cdot A \cdot \Delta T \tag{33}$$

$\alpha$        heat transfer coefficient, $[\alpha] = 1 \dfrac{W}{m^2 K}$

$A$        surface, $[A] = 1\ m^2$

$\Delta T$        difference in temperature, $[\Delta T] = 1$ K

Elisabeth Hufnagl

The dimensionless representation of $\alpha$ is the Nusselt Number $Nu$ given in Equation 34.

$$Nu = \frac{\alpha \cdot L}{\lambda} \qquad (34)$$

$Nu$      Nusselt Number

$\alpha$      heat transfer coefficient, $[\alpha] = 1 \frac{W}{m^2 K}$

$L$      significant length, $[L] = 1$ m

$\lambda$      thermal conductivity, $[\lambda] = 1 \frac{W}{Km}$

There is an essential difference between forced convection and free convection. For analysis concerning forced convection, the Reynolds Number $Re$ is the significant property. The analysis given in section 5.2.3 obtains a solution for the heat transfer with free convection.

The free convection is defined by the dimensionless Grashof Number $Gr$ and the characteristic material property given by the Prantl Number $Pr$. The Nusselt Number for free convection is derived from the Grashof Number and the Prantl Number. The former is significantly defined by the evaluated body's dimension (significant length) and the mediums thermal properties. The latter is derived from material characteristics, which are usually given in tables.

$$Nu = f\{Gr, Pr\} \qquad (35)$$

$$Gr = \frac{L^3 \cdot g \cdot \beta \cdot \Delta T}{\nu^2} \qquad (36)$$

$$Pr = \frac{\nu}{a} \qquad (37)$$

$$a = \frac{\lambda}{\rho \cdot c_p} \qquad (38)$$

$Gr$      Grashof Number

$L$      significant length, $[L] = 1$ m

$g$      earth acceleration, $[g] = 1 \frac{m}{s^2}$

$\beta$      thermal expansion coefficient, $[\beta] = 1 \frac{1}{K}$

$\nu$      kinematic viscosity, $[\nu] = 1 \frac{m^2}{s}$

$a$        temperature conductivity, $[a] = 1 \ \dfrac{m^2}{s}$

$\lambda$        thermal conductivity, $[\lambda] = 1 \ \dfrac{W}{Km}$

$\rho$        density, $[\rho] = 1 \ \dfrac{kg}{m^3}$

$c_p$        specific thermal capacity at constant pressure, $[c_p] = 1 \ \dfrac{J}{kgK}$

For specific problems in the calculation of free convection the Rayleigh Number is a frequently used factor. It is defined as $Ra = Gr \cdot Pr$. For its calculation the material characteristics for a mean value $\dfrac{T_1 + T_2}{2}$ of the temperatures given in the specific arrangement are to be used.

**The thermal radiation** is energy, which is emitted to the environment by electromagnetic waves. It is not bound to a medium (e.g. a fluid). The greater the temperature of an object, the greater the thermal radiation.

The energy flux density $\dot{e}_s$ is defined as given in Equation 39.

$$\dot{e}_s = \sigma \cdot T^4 \tag{39}$$

$\dot{e}_s$        energy flux density, $[\dot{e}_s] = 1 \ \dfrac{W}{m^2}$

$\sigma$        Stefan Boltzmann constant, $\sigma = 5.67 \cdot 10^{-8} \dfrac{W}{m^2 K^4}$

$T$        temperature, $[T] = 1 \ K$

The emitted thermal radiation of real objects is scaled by the degree of emission $\varepsilon$ ($\varepsilon$ varies between zero and one). Therefore, the energy flux density becomes:

$$\dot{e} = \varepsilon \cdot \dot{e}_s = \varepsilon \cdot \sigma \cdot T^4 \tag{40}$$

### 5.2.3   Analytic Approach to Thermic Stress Assessment

The physical relationships used for the calculations in this sections were found in [39] and in [40].

Power resistors used for neutral point treatment often consist of vertical plates, which are arranged parallel to each other, as visible in Figure 26.
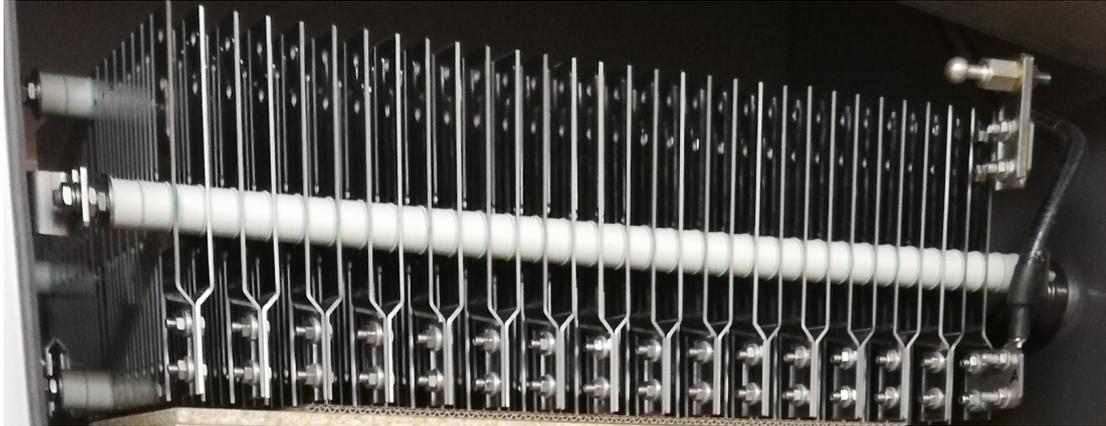
Figure 26: Detail view of LONE resistor

Usually the resistor is placed in a metal housing. A detailed analytic calculation of the heatflow for such an arrangement exceeds this thesis' boundaries.

Therefore, the heating behaviour of the resistor is calculated for a solid cube according to *Model 1* (see section 5.2.1).

Instead of plates parallel to each other, the total volume of those plates is estimated based on the following assumptions:

- the resistor consists of 15 iron plates

- each plate measures 5 mm in width, 60 mm in depth and height

- the resistance of the arrangement is 16 Ω

The volume resulting from these assumptions is used for the calculation of the measures of an equivalent cube. The following properties are evaluated:

- temperature rise due to the detection current proposed in [37]

- acceptable operation duration

- minimal lag time for sufficient cooling down without forced cooling

**Calculation of the heating behaviour**

As a first step, the operation duration, until the maximum temperature rise of the resistor is reached is calculated. The maximum temperature rise is assumed to be between 200°C and 300°C by the author.

$$\Delta t = \frac{c_{Fe} \cdot \rho_{Fe} \cdot V_{Fe} \cdot \Delta T}{R_{neutral} \cdot I_{detection}^2} \tag{41}$$

$\Delta t$       operation duration in seconds

$c_{Fe}$       specific thermal capacity of iron, $[c] = 1 \, \dfrac{J}{kgK}$

$\rho_{Fe}$      density of the material, $[\rho]{=}1 \; \dfrac{kg}{m^3}$

$V_{Fe}$      volume of the iron cube, $[V]{=}1 \; m^3$

$\Delta T$      temperature rise in K

$R_{neutral}$    resistance of system neutral resistor

$I_{detection}$   detection current according to protection design

The calculation of $\Delta t$ according to Equation 41 is acceptable for a very small span of time. Therefore, this approach is limited to only a few seconds. As shown in Figure 27, the operation time of one second, proposed in [37], is reached at a maximum temperature rise of 220°C.
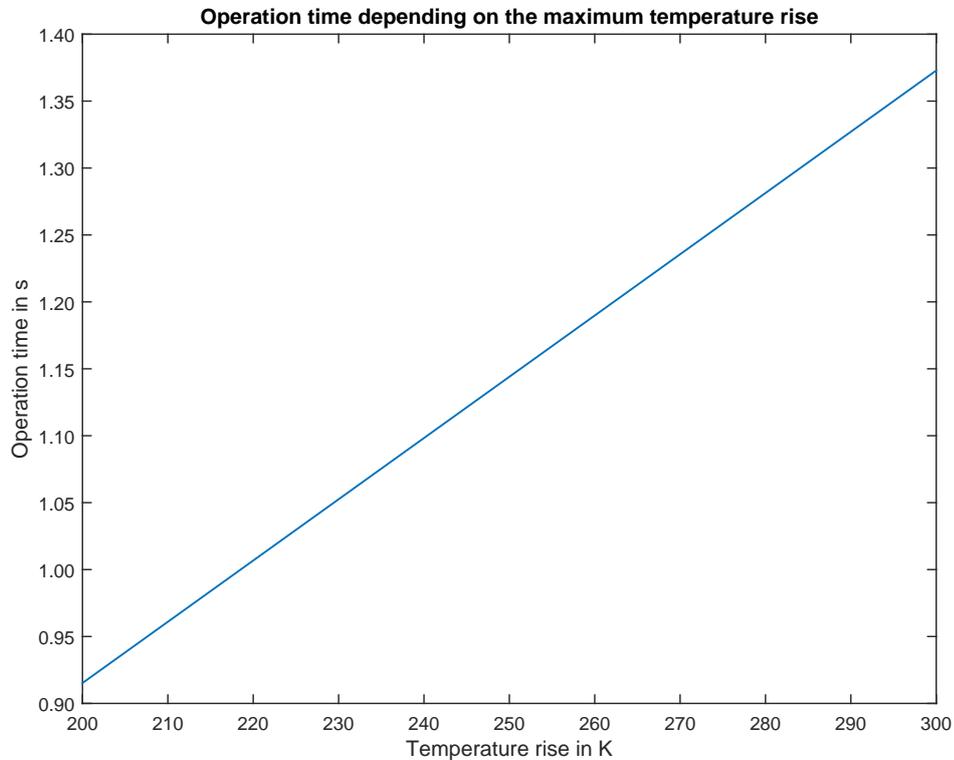


Figure 27: Operation time depending on the maximum temperature rise

The temperature rise depends on the energy absorption $\Delta E$ of the resistor. Under the assumption, that the entire active power caused by the detection current flows into the iron cube, $\Delta E$ equals the work $W$ (see Equation 30). With an operation duration of one second ($\Delta t = 1s$), the work $W$ equals the active power $P = R_{HPE} \cdot I_{HPE}^2$ (see Equation 42). Possible changes in the system neutral resistance due to the temperature rise are neglected in this engineering approach.

$$\Delta E_{Cube} = W = R_{neutral} \cdot I_{detection}^2 \cdot \Delta t \qquad (42)$$

$\Delta E_{Cube}$    change of energy within the cube

$W$    work

$R_{neutral}$    resistance of system neutral resistor

$I_{detection}$    detection current according to protection design

$\Delta t$    operation duration in seconds

Based on the first fundamental law of thermodynamics, the temperature rise can be calculated as given in Equation 43:

$$\Delta T = \frac{\Delta E_{Cube}}{c_{Fe} \cdot \rho_{Fe} \cdot V_{Fe}} \tag{43}$$

$\Delta T$    temperature rise

$\Delta E_{Cube}$    change of energy (here: increase) within the cube

$c_{Fe}$    specific thermal capacity of iron, $[c] = 1 \ \dfrac{J}{kgK}$

$\rho_{Fe}$    density of iron, $[\rho] = 1 \ \dfrac{kg}{m^3}$

$V_{Fe}$    volume of the iron cube, $[V] = 1 \ m^3$

The approximation of $\Delta T$ according to Equation 43 for $\Delta t = 1s$ (one second of operation) results 218.5 K. Starting from an ambient temperature of 25°C, this entails a maximum temperature of 243.5°C.

Due to thermal convection and radiation, the maximum temperature of the iron cube should be reduced. The following calculations show the limitation of the convection's impact on the maximum temperature. The heat transfer coefficient $\alpha$ is calculated via Equation 34 from the Nusselt Number and the significant length as well as the thermal conductivity $\lambda$. According to [39], the Nusselt Number of a cube can be derived from Equation 44.

$$Nu = 5.748 + 0.752 \cdot \left( \frac{Ra}{f_4(Pr)} \right)^{0.252} \tag{44}$$

$Nu$    Nusselt Number

$Ra$    Rayleigh Number defined in Equation 45

$f_4$    function defined in Equation 48

$$Ra = \frac{\beta \cdot g \cdot \Delta T \cdot L^3}{\nu \cdot \kappa} \tag{45}$$

$$L = \frac{A}{D} \tag{46}$$

$$D = \frac{2 \cdot s}{\sqrt{\pi}} \tag{47}$$

$\beta$    thermal expansion coefficient, $[\beta]= 1 \; \dfrac{1}{K}$

$g$    earth acceleration

$\Delta T$    temperature rise

$L$    significant length

$\nu$    kinematic viscosity, $[\nu]= 1 \; \dfrac{m^2}{s}$

$\kappa$    temperature conductivity, $[\kappa]= 1 \; \dfrac{m^2}{s}$

$A$    surface of the cube

$s$    edge length of the cube

Equation 47 is valid, if one side of the cube is parallel to the horizontal plane. Otherwise, D has to calculated with $D = \sqrt{\dfrac{4 \cdot A_{proj}}{\pi}}$ (for details see [39]).

$$f_4(Pr) = \left( 1 + \left( \frac{0.492}{Pr} \right)^{\frac{9}{16}} \right)^{\frac{16}{9}} \tag{48}$$

$Pr$    Prantl Number

With $\alpha$ obtained with the help of the equations above, the heat flow $\dot{Q} = \alpha \cdot A \cdot \Delta T$ due to convection can be calculated. $A$ equals the surface of the equivalent iron cube, $\Delta T$ once more depends on the resistor specification. For a $\Delta T = 220K$ (which corresponds with the operation time of one second), the heat flow reaches 644.4 W; that is 0.003 percent of the active power causing the rise of temperature. Therefore, the negligence of the convection for a first estimation of the heat built-up seems acceptable. Still it should be kept in mind, that the main reason for the quite low percentage of convection is the very limited surface of a solid cube in comparison to an arrangement of parallel plates.

This also applies for thermal radiation (see Equation 40). The emitted thermal radiation of a metallic object due to a temperature of 243.5°C is limited to around 1212 $\dfrac{W}{m^2}$. Therefore, the equivalent cube would only emit around 654.5 W by thermal radiation. If the actual surface of the parallel plates of the HPE resistor are used for the calculation of the thermal radiation, it reaches around 13.3 kW. Therefore, the thermal radiation is negligible for this type of evaluation.

## Calculation of the cooling behaviour

In order to estimate the appropriate lag time of the system neutral resistor, the thermal time constant $\tau$ is assessed. The thermal time constant is the product of the thermal resistance (see Equation 49) and the thermal capacity (see Equation 50) of the arrangement.

$$R_{therm} = \frac{1}{\alpha \cdot A} \tag{49}$$

$R_{therm}$     thermal resistance

$\alpha$     heat transfer coefficient, $[\alpha] = 1 \, \dfrac{W}{m^2 K}$

$A$     surface, $[A] = 1 m^2$

$$C_{therm} = c_{Fe} \cdot \rho_{Fe} \cdot V_{Fe} \tag{50}$$

$C_{therm}$     thermal capacity

$c_{Fe}$     specific thermal capacity of iron, $[c] = 1 \, \dfrac{J}{kgK}$

$\rho_{Fe}$     density of iron, $[\rho] = 1 \, \dfrac{kg}{m^3}$

$V_{Fe}$     volume of the iron cube, $[V] = 1 \, m^3$

To provide a rather simple solution, in a first approach the thermal resistance and capacity of the solid cube are used to determine $\tau$ (*Model 1*). As shown in Figure 28, this leads to an unrealistic high cooling time of 22.76 hours (time until the cube reaches the ambient temperature of 25°C).

In a second approach, the actual surface of the arrangement was taken into account (*Model 2*), as the ratio between the surface of the cube and the actual surface equals 20.33 (see 'Approximation for parallel plates' in Figure 28). The cooling time derived from this is calculated as 1.12 hours. From the first to the second draft, $\tau$ was reduced from around 10 hours to half an hour.
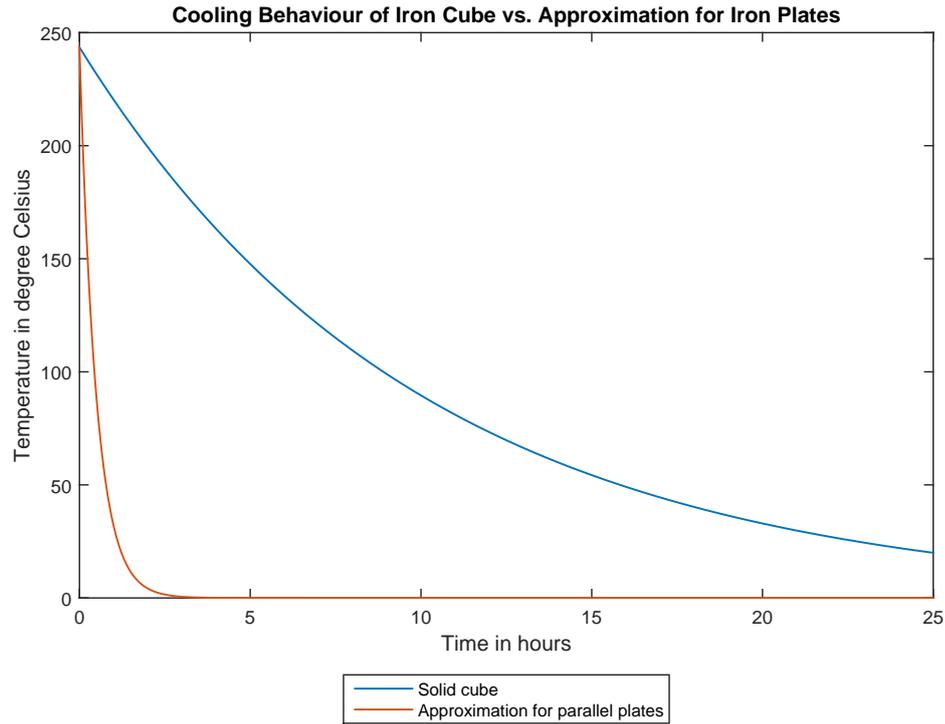
Figure 28: Cooling behaviour of a solid iron cube in comparison to the estimated cooling behaviour of an arrangement of parallel plates

As the heat transfer coefficient $\alpha$ used for the *Model 2* approach is derived from the Nusselt Number and the significant length of a cube, there is a calculation error in the approximation according to *Model 2*.

In order to validate the estimation above, the cooling behaviour of a single vertical plate is determined (*Model 3*). Therefore, the Nusselt Number of a vertical surface is calculated according to Equation 51, [39]:

$$Nu = \left(0.825 + 0.387 \cdot (Ra \cdot f_1(Pr))^{\frac{1}{6}}\right)^2 \tag{51}$$

$Nu$      Nusselt Number

$Ra$      Rayleigh Number defined in Equation 45

$f_1$      function defined in Equation 52

$$f_1(Pr) = \left(1 + \left(\frac{0.492}{Pr}\right)^{\frac{9}{16}}\right)^{-\frac{16}{9}} \tag{52}$$

The new heat transfer coefficient $\alpha$ is calculated by the use of Equation 34. The thermal resistance $R_{therm} = \dfrac{1}{\alpha \cdot A}$ is assessed under negligence of the top-, bottom-, front- and back-face of the plate.

Therefore, there is still more surface available for cooling purposes. On the other hand, the heat build-up between the parallel plates, which potentially worsens the cooling behaviour of the arrangement, is not taken into account in this estimation. As the thermal resistance is derived from the measures of one single plate, also the thermal capacity is adjusted to the new setting. The thermal constant $\tau$ is calculated as 0.32 hours. This results in a cooling time of 0.73 hours, as shown in Figure 29.
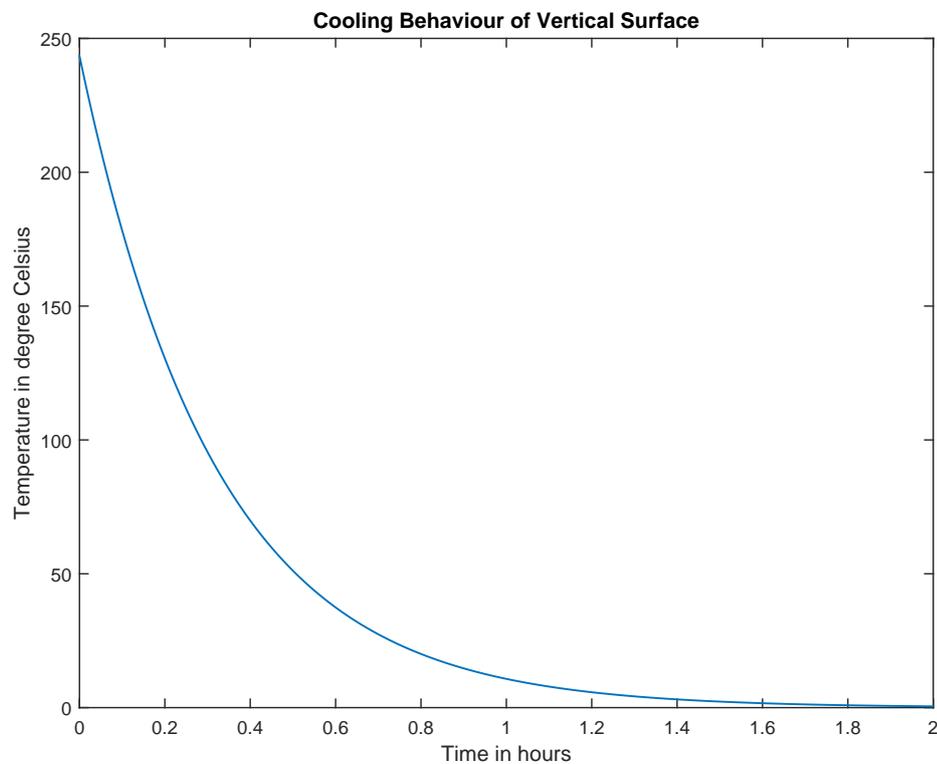


Figure 29: Approximated cooling behaviour of a single plate

## Conclusions from the Analytic Approach to Thermic Stress Assessment

- The temperature rise due to the detection current proposed in [37] for an operation time of one second reaches 218.5 K, if a reduction by convection or radiation is neglected.

- The proposed operation time of one second is sensible for a temperature rise

strictly limited to 220 K. If resistor specifications allow a higher temperature rise of e.g. 300 K, a limited extension of operation time should be possible.

- A realistic approximation of the lag time is hard to achieve, as the thermal resistance of a solid cube (*Model 1*) results in an exceedingly high thermal time constant. This is the result of a very limited surface, compared to parallel plates, which also limits the convection to a rather unrealistic low level of 644.4 W.

  As for the first few seconds of the heating process, the convection as well as the radiation can be neglected (as all the energy is absorbed by the material, thermal capacity respectively), the achieved results for $\Delta t$ and $\Delta T$ seem sensible. The heating process is considered adiabatic, as the heatflow caused by free convection and thermal radiation reaches only 0.006 percent of the active power causing the temperature rise (*Model 1*). Henceforth the thermal radiation and the thermal conduction are neglected in this engineering approach.

  For the cooling behaviour, however, the actual surface is a key factor. As the thermal resistance is inversely proportional to the surface as well as $\alpha$, the simple model of a solid cube is not sufficient any more. In consequence of the factor $\alpha$ being derived from the Nusselt Number and the significant length, which have been determined for a cube, it should not be used for the calculation of the thermal resistance of an arrangement of parallel plates (Model 2).

  Nevertheless, for a first, cautious, estimation on the cooling behaviour, the use of $\alpha$ for a cube combined with the surface of an arrangement of parallel plates results in a longer cooling time, than the estimation of one single plate (*Model 3*) considering only the sides and neglecting the top, bottom, front and back. The ratio of around 1.53 results in a rather cautious time estimation.

  The final determination of the lag time needed for a cool down to ambient temperature according to *Model 3* confirms the initial suspicion of a rather cautious setting of the lag time of the resistor in [37] (HPE method), especially as thermal radiation is neglected in this approach. Still there are several uncertainties in the approach shown above.

  Therefore, the proposed lag time of one hour remains a sensible choice.

- As a final remark to this section it should be mentioned, that even though the second (*Model 2*) and the third approach (*Model 3*) to cooling time estimation differ from another in terms of thermal time constant (factor

$\approx 1.6$) and cooling time (factor $\approx 1.5$), still there is even more noticeable difference in heat flow caused by convection (factor 2, see Figure 30).
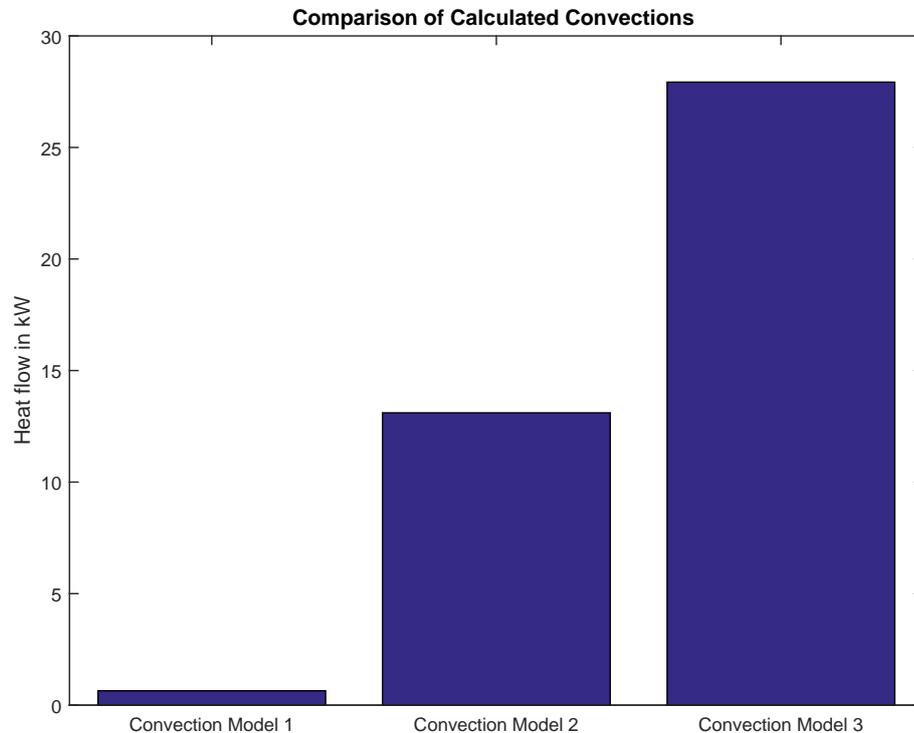


Figure 30: Comparison of calculated convections for the proposed engineering approaches

### 5.2.4 References to Manufacturer Specifications

As has become clear in section 5.2.3, detailed information on the dimensions, as well as material specifications are the key to a well informed estimation of the heat flow of electrical equipment parts. Fortunately, a search for resistor specifications allowed some insight on a manufacturer's guidelines on power resistor operation and heat flow. An example operations ranges assigned to temperatures and rates of energy dissipation is shown in Figure 31.
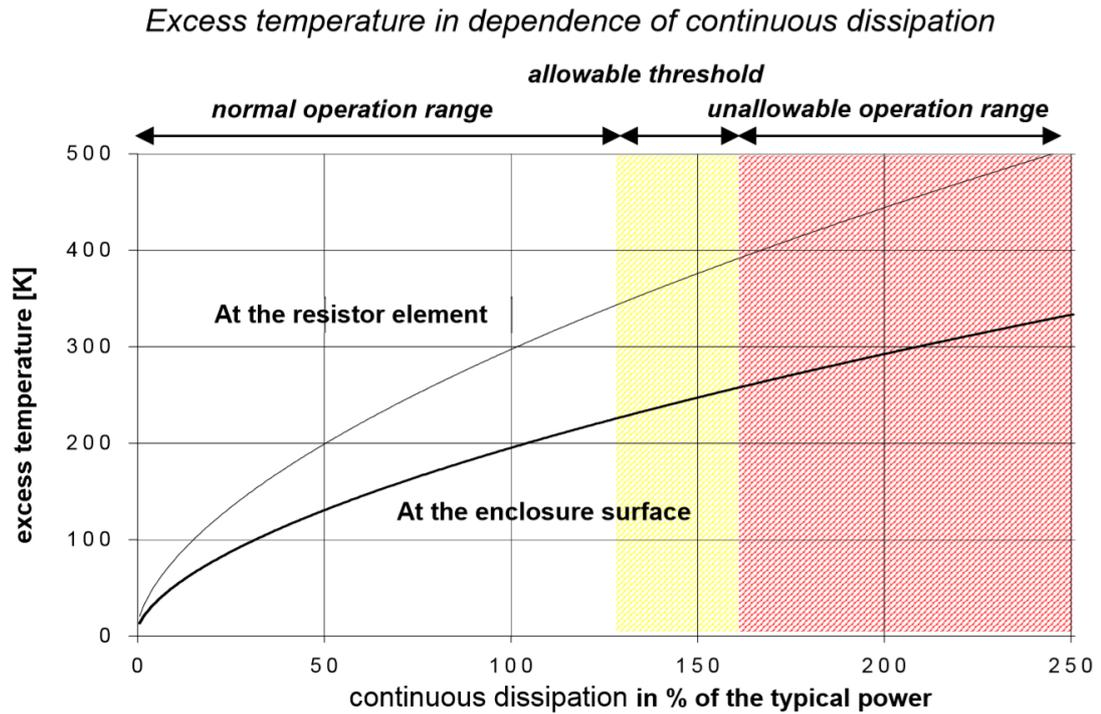
Figure 31: Manufacturer specification of excess temperature over the continuous power in percent of the listed (typical) power, image quoted from [41]

The figure above may not apply to all power resistors used for neutral point treatment, still it provides an acceptable reference for pre-evaluations aside from detailed heat flow calculations (which would probably be accomplished by Finite Element Analysis).

# 6 Risk Assessment

For a better introduction to this topic, the pros and cons of the two mainly pursued operation philosophies are summarized in section 6.1.

One compelling argument to find a suitable solution for the network in question is repeated and discussed in section 6.2.

The risk of EPR is the topic of several working groups and PhD theses. In section 6.3 the approach presented in the British Standard of EN 50522 ([36]) is shown in its outlines.

Finally the avoidance of Penalty Payments is addressed in section 6.4

## 6.1 Continued Operation vs. Immediate Tripping

In many medium voltage networks with earth fault compensation, continued operation during phase-to-earth faults is considered as best practice. However, this approach can lead to subsequent faults in networks with a high percentage of aged cable structures, whose repair as a consequence is complex and therefore time-consuming. Thus immediate tripping can become an attractive operation mode if reliability indices are substantial, as outage times due to subsequent faults can easily exceed those of tripped single earth faults.

An example for this was published in [5] and [6], describing an existing urban MV network. In the mentioned network, the average interruption duration caused by earth faults was one hour. For customers affected by a subsequent earth fault the interruption duration is increased by another hour. Every further (i++) earth fault in other semi-rings of the network inflicts an interruption duration of one hour plus i hours for the customers in this particular branch. As fifty percent of single earth faults lead into double- or even multiple earth faults ([6]), average interruption durations reach considerable dimensions. This high rate of single-pole faults developing into multi-pole failures may seem high compared to other urban areas such as Helsinki (24%) or Dresden (35%) [7], still it corresponds with experiences of an Austrian DSO. As the average interruption frequency of LONE is nearly the same as with resonant grounding systems, non-availability should easily be cut in half [6].

## 6.2 Risk of Cross-Country-Faults in Aged Cable Structures

The risk of cross-country-faults rises with every stress on aged cable structures exceeding the usual boundaries of operation. The continued operation of a line-

to-ground fault causes an increase of the line-to-ground voltage by $\sqrt{3}$.

If the insulation of the cables is already damaged by e.g. water trees, electrical trees respectively, the remaining insulation may break down, leading to a further fault. The second earth fault, caused by this, may root in another part of the network, causing a more complicated fault detection and restoration of operation. Therefore, the restoration time increases considerably.

As penalty payments are being considered more frequently, the amount of ENS becomes an important impact factor, depending on the assumed cost (e.g. $10 \, €/\text{kWh}$) not to be neglected. [42]

One way to avoid cross-country-faults would be the immediate tripping of phase-to-earth faults, instead of continuing the operation (which would be the standard procedure). Statistics of the 10-kV-network in Helsinki show, that the majority of multi-pole earth faults arise within a few minutes from the initial earth fault [7].

By accepting possible setbacks concerning ASIDI (which should be investigated beforehand) and local increases of non-availability, to keep the material damage as small as possible and to lower the probability of multiple failures. If a change of neutral point treatment is pursued, a close analysis of several impact factors including the effect on availability indices is necessary.

### 6.2.1 Impact Factors on the Non-availability in Earth Fault and Cross-Country-Fault Scenarios

The aim of this section is to assess, which network-specific impact factors involve significant disadvantages for resonant grounded network structures concerning the availability regarding earth fault and cross-country-faults.

In order to find the relation between the

- total number of earth faults

- rate of double earth faults

- restoration durations depending on the fault location of the second earth fault

    - in the same half loop

    - in the other half loop of the same loop

    - in another ring of the network

...and the resulting non-availability, the load-weighted non-availability respectively, an exemplary calculation for the following network is done.

The network shown in Figure 32 consist of $\alpha$ open loops. Each feeder is $\beta$ kilometres long. The network's total load installed is $\gamma$ kVA. The load is assumed to be evenly distributed, therefore every half loop supplies the same load of $\delta = \dfrac{\gamma}{2 \cdot \alpha}$ kVA.
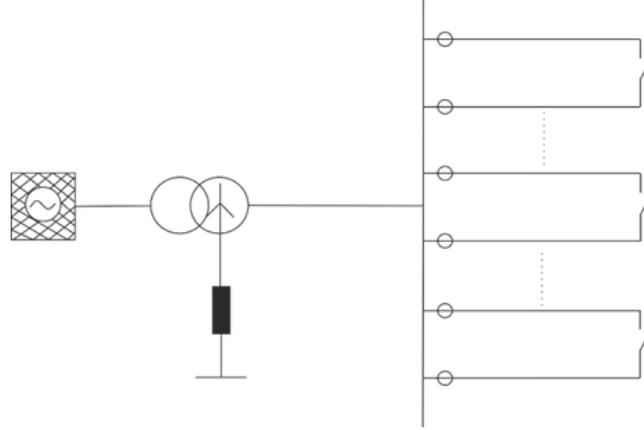


Figure 32: Network structure for the analysis of the non-availability due to single and double earth faults

The non-availability $Q$ is defined as the product of the interruption frequency $H$ and the corresponding interruption duration $t_{interr}$. In order to indicate the impact of earth fault induced interruptions to the overall network, a load-weighted non-availability $Q_{S,e/f,RG}$ is defined according to Equation 53.

$$Q_{S,e/f,RG} = \frac{h_{e/f} \cdot d_1 \cdot \delta + h_{e/f} \cdot r_{double,e/f} \cdot (d_{1,d-e/f} + d_i) \cdot S_{Seg,i}}{\gamma} \qquad (53)$$

$Q_{S,e/f,RG}$  load-weighted non-availability due to a specific earth fault / cross-country fault scenario

$h_{e/f}$  frequency of earth fault induced interruptions per feeder

$d_1$  interruption duration for single earth faults in resonant grounded networks; caused by switching actions

$\delta$  load per half loop

$r_{double,e/f}$  rate of earth faults developing into cross-country-faults (double earth faults respectively)

$d_{1,d-e/f}$  interruption duration for the first earth fault in double earth fault scenario for resonant grounded networks

$d_i$  interruption duration for the second earth fault depending on its location in double earth fault scenario for resonant grounded networks

$S_{Seg,i}$      load of disconnectable feeder segment, depending on location of second earth fault

$\gamma$      total load installed in assessed network

Index i of $d_i$ and $S_{Seg,i}$ depending on location of second earth fault:
i=2    second earth fault in other ring
i=3    second earth fault in respective other half loop (same ring)
i=4    second earth fault in same half loop

The obtained non-availabilities are compared to the non-availability of a Low Ohmic Neutral Earthing network with immediate tripping.

As in LONE networks, cross-country-faults do not occur, the calculation of the load-weighted non-availability is reduced to Equation 54.

$$Q_{S,e/f,LONE} = \frac{h_{e/f} \cdot d_{1,d-e/f} \cdot S_{Seg}}{\gamma} \tag{54}$$

For this analysis an interruption frequency due to single earth faults $H_{e/f} = \dfrac{0.77}{100km \cdot yr}$ is defined as the starting value. The rate of earth faults developing into double earth faults ($r_{double,e/f}$) is assumed to equal fifty percent as a starting value. All interruption durations are varied.

### 6.2.2    Results to the Variation of Impact Factors on Non-availability

Calculation details and starting values for the following analysis are listed in the appendix (see section 8.2).

**Variation of the earth fault induced interruption frequency**

As shown in Figure 33, the non-availability due to single earth faults and cross-country-faults increases strictly linear with the interruption frequency $H_{e/f}$. The non-availability of the RG network increases with the same incline for each fault location for the second earth fault, because each restoration duration was assumed to be the same for this analysis (see Table 12). The load-weighted non-availabilities vary from each other depending on the fault location because the interrupted load used for the weighting depends on the fault location. The worst-case scenario is the respective other half loop as the fault location for the second earth fault.

The incline of the non-availability of the LONE network ($Q_{LONE}$) is smaller than the incline of the non-availability of the RG network ($Q_{RG}$). The same applies to the load-weighted non-availability.
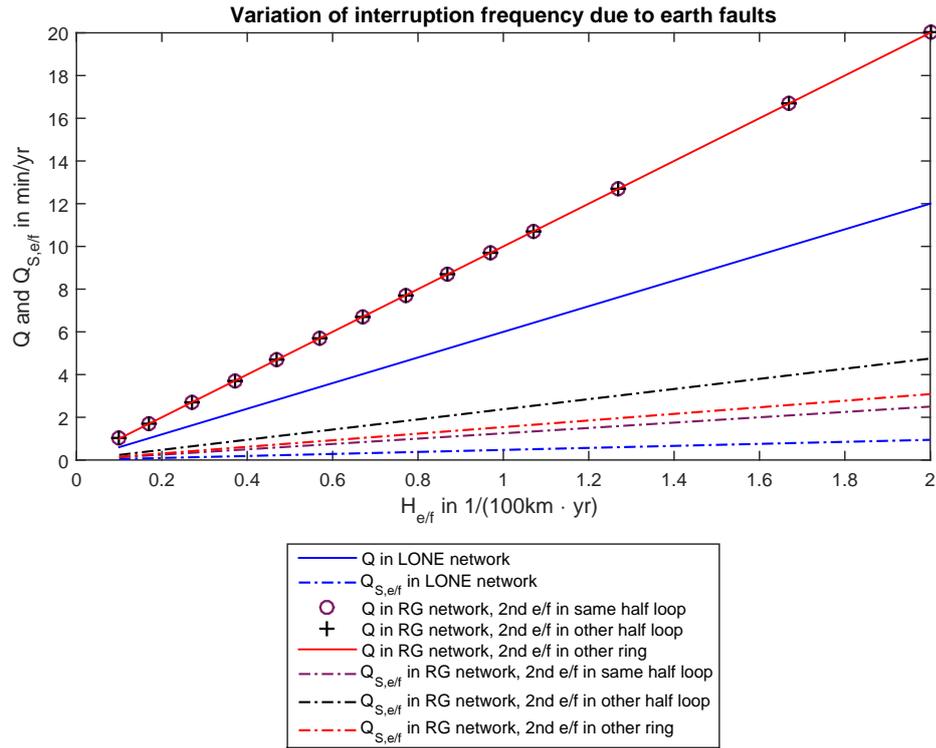
Figure 33: Influence of $H_{e/f}$ on $Q$ and $Q_{S,e/f}$ for LONE and RG networks

## Variation of the double earth fault rate

As earth fault (e/f) currents in LONE networks magnitudes comparable to short circuit currents, they are interrupted with low switching times. Therefore, cross-country-faults do not occur in LONE networks, entailing a constant non-availability shown in Figure 34.

Non-availabilities in RG networks increase linearly with the double earth fault rate. The non-availabilities cross at a certain double earth fault rate, marking the point at which - concerning earth fault induced non-weighted non-availabilities - LONE networks offer higher availability than RG networks. For this specific example, this point is at 28 %. Of course, the incline of the graph is sensible to the interruption durations assumed (see Table 12).

The load-weighted non-availabilities cross at an even lower double earth fault rate. In this example the rate is 10 %. Again, the balancing-point is highly sensible to the assumed impact factors such as interrupted load and interruption durations.
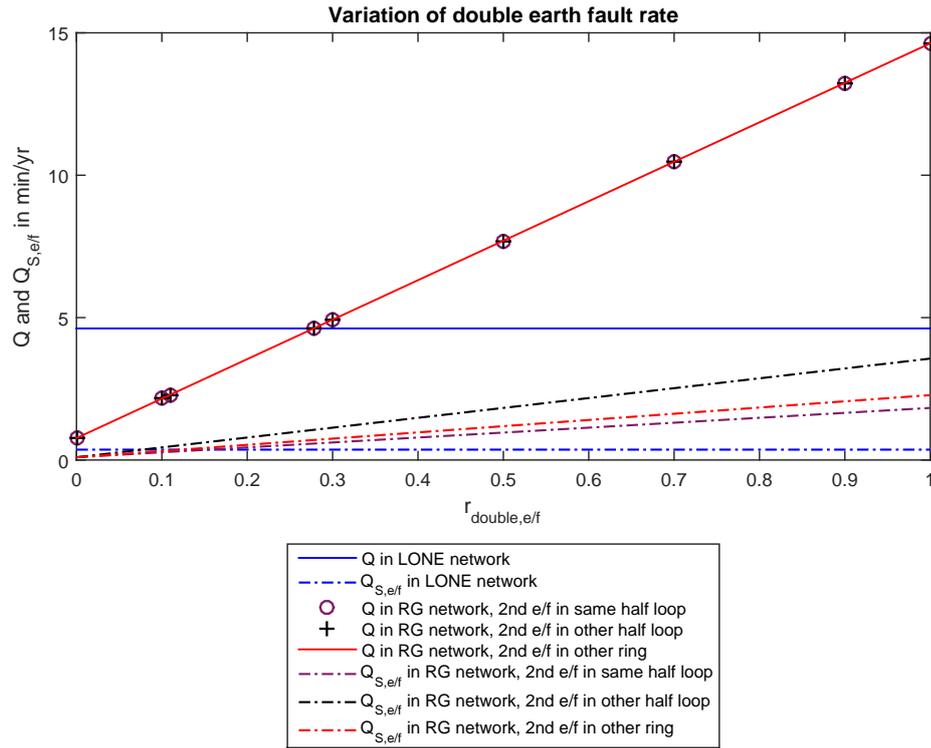
Figure 34: Influence of $r_{double,e/f}$ on $Q$ and $Q_{S,e/f}$ for LONE and RG networks

## Variation of the interruption duration of the first earth fault in double earth fault scenario

In Figure 35, the non-availabilities of LONE and RG networks cross at an interruption duration of 2 hours and 21 minutes. Thus for interruption durations of the first earth fault longer than 2.3 hours (in this specific example), LONE networks do not offer advantages in terms of non-weighted availability concerning earth fault scenarios.

The load-weighted non-availabilities, on the other hand, cross after around nine hours.

A further effect of a change in system neutral treatment from RG to LONE is the steeper rise of the non-availability in LONE networks for increasing interruption durations $d_{1,d-e/f}$ compared to RG networks. Then again the load-weighted non-availabilities (worst-case scenario excepted) hardly vary from each other.
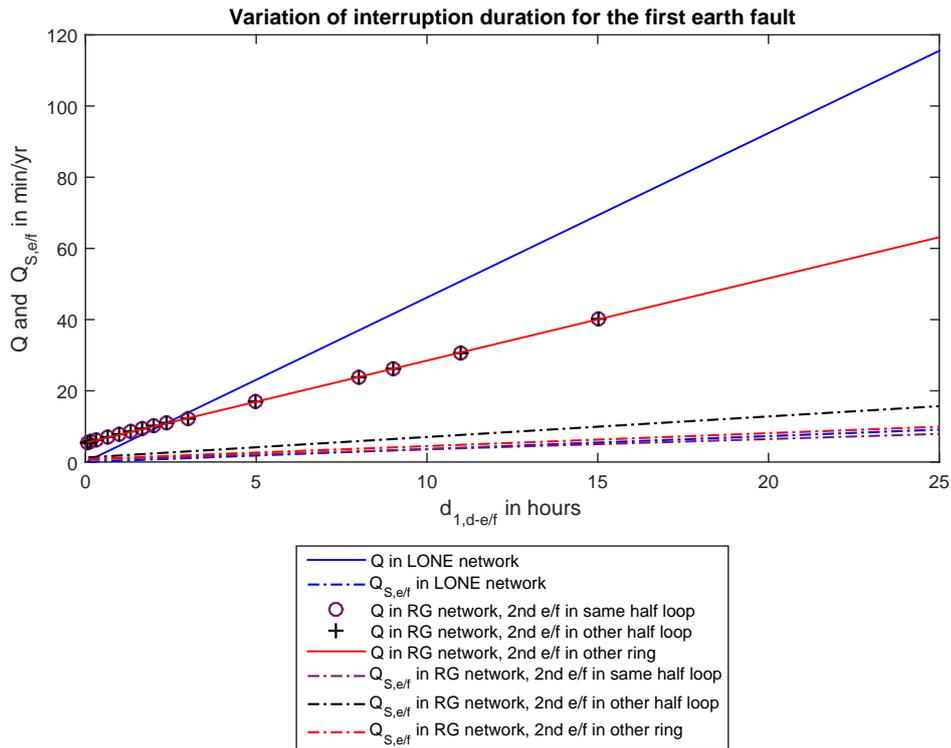
Figure 35: Influence of $d_{1,d-e/f}$ on $Q$ and $Q_{S,e/f}$ for LONE and RG networks

## Variation of the interruption duration of the second earth fault in double earth fault scenario depending on the fault location

The variation of the interruption durations $d_2$, $d_3$ and $d_4$ (see Figure 36, Figure 37 and Figure 38) shows the linear behaviour of the respective non-availabilities and load-weighted non-availabilities for each fault location for the second earth fault. As cross-country-faults do not occur in LONE networks, the respective non-availability remains constant in each parameter variation.

Figure 36 shows the variation of the interruption duration due to a second earth fault in another ring of the network.
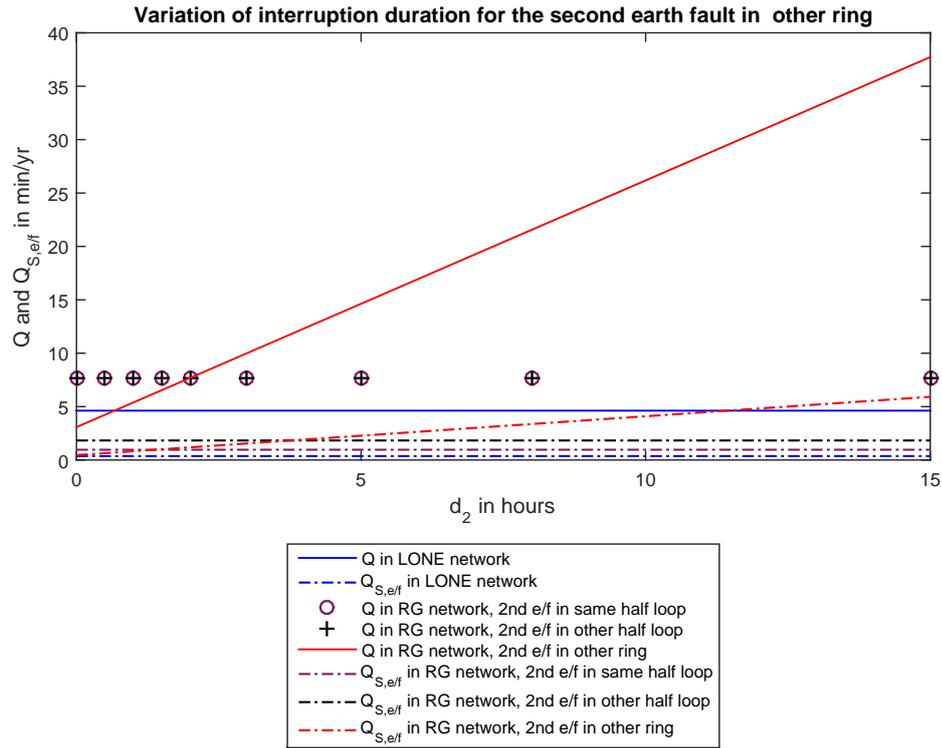
Figure 36: Influence of $d_2$ on $Q$ and $Q_{S,e/f}$ for LONE and RG networks

Figure 37 shows the variation of the interruption duration due to a second earth fault in the other half loop of the same ring in the analysed network. This fault location represents the worst-case scenario for cross-country faults, as there remains no restoration option based on implemented switching options. Thus, the whole ring is affected resulting in the highest interrupted load.
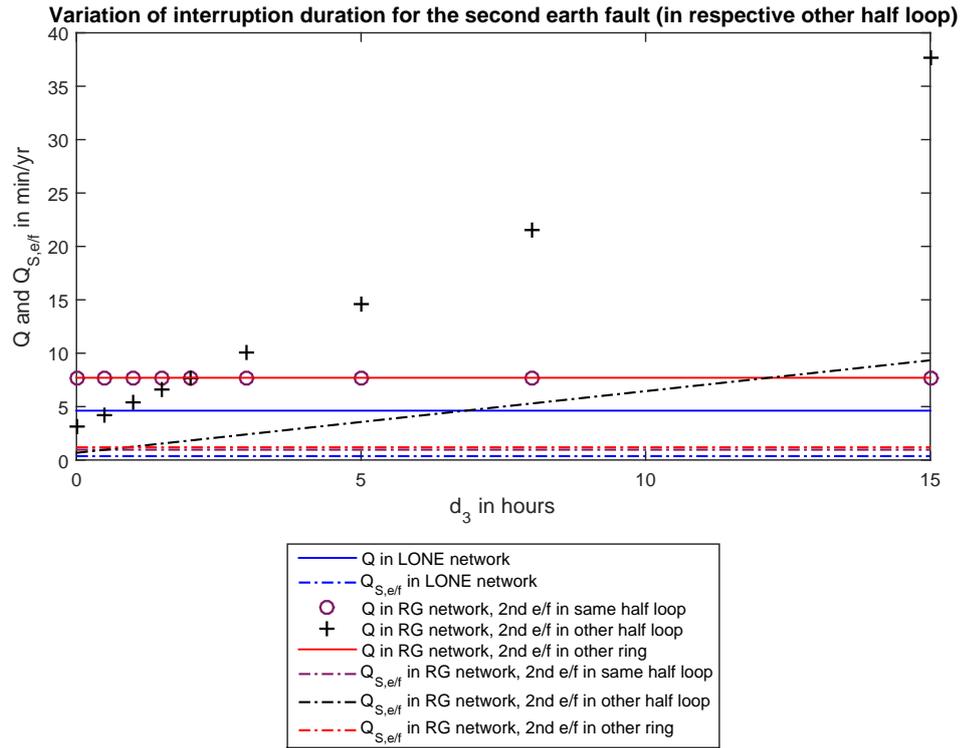
Figure 37: Influence of $d_3$ on $Q$ and $Q_{S,e/f}$ for LONE and RG networks

Figure 38 shows the variation of the interruption duration due to a second earth fault in the same half loop of the network.
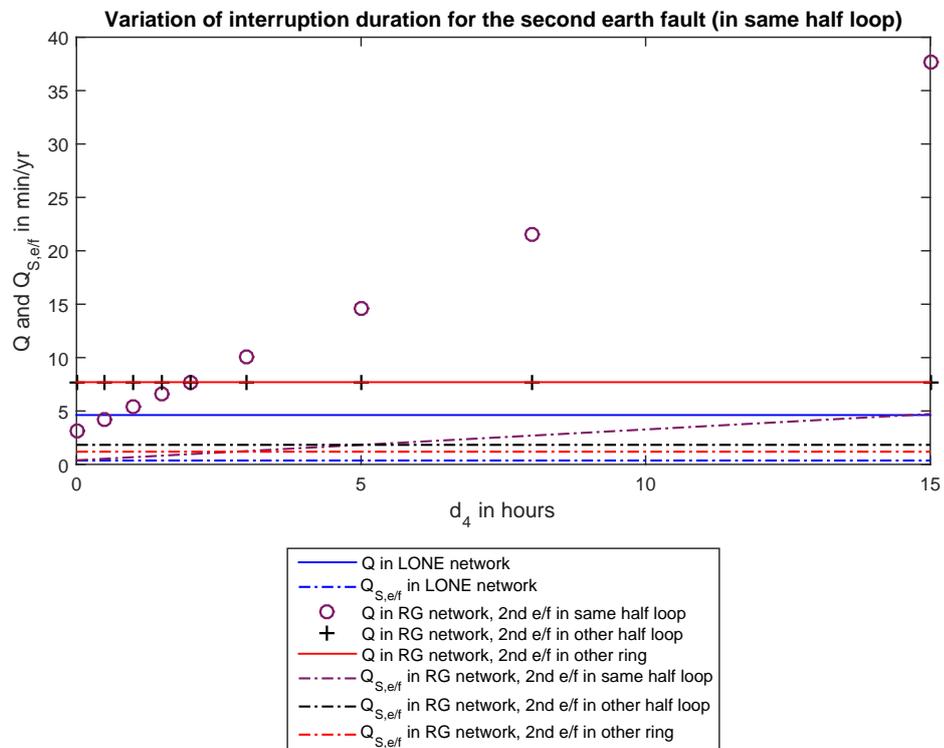


Figure 38: Influence of $d_4$ on $Q$ and $Q_{S,e/f}$ for LONE and RG networks

## 6.3 Risk of Danger by EPR

Several earth fault detection methods use a high current, which can lead, depending on local grounding, to a critical EPR. The effects of EPR on potential personal risks have to be analysed closely. If there is a verifiable global earthing system, according to current standards (EN 50522, [36]), no further investigations are necessary, as the compliance to step- and touch voltage limits is required per definition. If the global earthing system can't be proven [43], appropriate measures as local insulation rating, control earth electrodes, barriers, etc. have to prevent hazards by EPR [44].

Some countries (GBR, AUS, NZL) perform risk-based assessments, which basically analyse the actual probability of an incident due to earth faults. If the probability exceeds a limit of $10^{-6}$ per year and person, a re-evaluation is required. In this case, the probability of a simultaneous occurrence of personal risk (due to EPR) and the actual touch of a conductive part carrying the risen potential by a person has to be calculated using the following Equation 55 .

$$p_{coinc} = \frac{f_n \cdot p_n \cdot (f_d + p_d) \cdot T}{365 \cdot 24 \cdot 60 \cdot 60} \cdot CRF \tag{55}$$

$p_d$      average duration of exposure

$f_d$      average duration of average earth fault leading to a critical EPR

$p_n$      rate at which exposures of a person occur

$f_n$      rate at which faults occur

$T$      number of years

$CRF$      coincidence reduction factor

The coincidence reduction factor is an empirical factor, which depends on the mitigation strategy. In [45] several examples for the coincidence reduction factor ($CRF$) are listed. Exemplary $CRF$ are given in Table 8.

Table 8: Examples for $CRF$ based on the mitigation strategy according to [45]

| Coincidence reduction method | $CRF$ |
|---|---|
| barrier fence | 0.1 |
| insulation covering | 0.4 |
| restricted access | 0.5 |
| install sign | 0.8 |

In [46] the fact of Equation 55 being a simple approximation is made clear. There are factors limiting the suitability of the formula to real life evaluations. The authors emphasise that the fault rate ($\lambda$ in the Poisson distribution) is bound to be

small in order to use the approximation. Unfortunately, until this time, there is no follow-up publication including an alternative expression for $p_{coinc}$.

There is a classification for the probability of coincidence given in Table 9, [45]:

Table 9: Individual Probability Limits, [45]

| Probability of coincidence | Classification and resulting implication |
|---|---|
| $p_{coinc} > 10^{-4}$ | high, intolerable risk; must prevent occurrence regardless of cost |
| $p_{coinc} = 10^{-6} - 10^{-4}$ | intermediate, ALARA region; must minimise occurrence unless risk reduction is impractical and cost are grossly disproportionate to safety gained. As Low As Reasonably Achievable (ALARA) |
| $p_{coinc} << 10^{-6}$ | low, tolerable risk |

## 6.4 Avoidance of Penalty Payments

The regulatory authority (Bundesnetzagentur (BNetzA) in Germany as well as e-control in Austria) as well as DSOs have been dealing with the possibility of an introduction of penalisation for a while by now. The German regulatory regime is already in force. In Austria a similar approach is being pursued.

The German approach is built around the so called Q-Element, which consists of the improvement of SAIDI (as a result of network restructuring or even development), the number of customers and a Monetary Factor ($MF$). This factor is derived from estimated interruption costs.

The Austrian version uses the load-based reliability index ASIDI. According to [47] the calculation of a customer-based reliability index is not possible, as there has not been a record of the number of customers affected by interruptions until now. By the introduction of smart meters to the Austrian electrical networks, this may change. Nevertheless the actual approach to a regulatory regime in Austria relies on ASIDI, for which statistic are available. As a result the $MF$ is derived from those costs, arising from the power not being supplied, which is referred to as value of lost load ($VOLL$). For the $VOLL$ several Austrian and German sources suggest €10.6/kWh . [48], [49], [50]

A dissertational thesis from Aalto University (Helsinki) suggests a quite similar $VOLL$ of €10/kWh for Finland. [42]

Finally, the Q-Element is calculated as given in Equation 56, [50]:

$$Q - Element = (ASIDI_{ref} - ASIDI_{act}) \cdot MF \cdot S_{inst} \tag{56}$$

$ASIDI_{ref}$    Reference-ASIDI

$ASIDI_{act}$    Actual ASIDI

$MF$           Monetary Factor

$S_{inst}$        Total transformer power installed in analysed network levels

The $MF$ is determined by the annual peak load of the network level considered (for the Austrian MV network it is network level 5), the total power of MV/LV transformers installed and the $VOLL$. It is calculated as given in Equation 57, [47]:

$$MF = \frac{S_{peak}}{S_{T,total}} \cdot VOLL \tag{57}$$

$S_{peak}$       annual peak load

$S_{T,total}$    total power of MV/LV transformers installed

$VOLL$    value of lost load

As $S_{peak}$ is assumed to be around 9500 MW and $S_{T,total}$ around 23900 MVA, the Austrian $MF$ is according to [50] considered to be around €0.07/(kVA min).
A further factor, which is often mentioned concerning this kind of analysis, is Cost of Energy not Supplied (CENS). It is calculated using the Energy Not Supplied (ENS), the non-availability and the $VOLL$. In order to achieve a regulatory regime which must not change the venue for the overall branch of industry an ASIDIQ (in addition to the actual ASIDI also planned interruptions are taken into account to a certain percentage, [50]) is drawn over the load densities as shown in Figure 39.
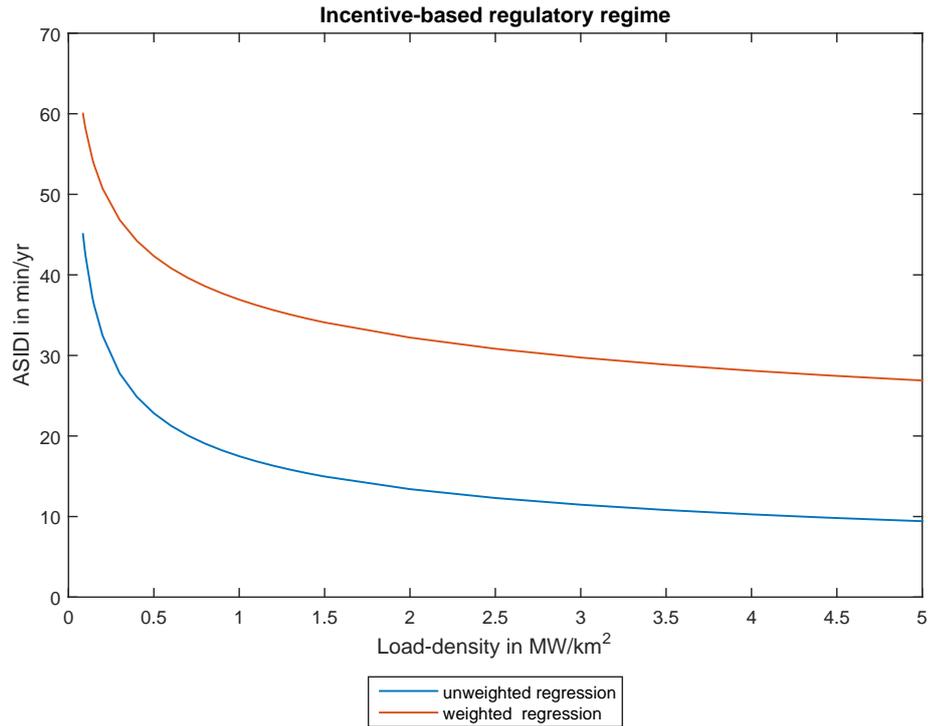
Figure 39: ASIDIQ over load-density, [50]

Afterwards the ASIDIQ-values of the DSO are drawn into the same diagram. Those, whose values are smaller than the given graph receive a bonus, which is financed by the malus of DSO whose values are bigger than the reference graph. Nevertheless, the particular reference value $ASIDI_{ref}$ should be regarded as a calculation tool, rather than a goal to reach as an incentive. The actual stimulus for DSO depends on the $MF$ and the achieved change of $ASIDI_{act}$ in reference to previous years.

This approach is meant to motivate DSO to invest into their network reliability at an early stage. In order to maintain the stimulus, reference values should be re-evaluated after a certain amount of time. Thus the reference graph changes with the same rate as the weighted[7] reliability level. [47]

The Austrian regulatory authority provides fault and interruption statistics. According to the statistics published on e-control's website, the Austrian average for ASIDI including unplanned events but excluding extraordinary events such as storms and catastrophies reached 22,19 $\dfrac{min}{yr}$ in 2016. [51]

In the previous year, e-control even distinguished between rural, intermediate and urban networks. Unfortunately, the most recent statistic does not include this

---

[7]In order to avoid a change of venue for the branch of industry, a weighted regression is being used. This is meant to ensure fairness, as bigger DSO expect higher bonuses or penalties

analysis. Therefore, to provide a better insight in Austrian relation concerning network reliability, the SAIDI of the year 2015 is given in Table 10.

Table 10: System Average Interruption Duration Index (SAIDI) of Austrian networks in 2015 depending on degree of urbanisation including unplanned events but excluding extraordinary events such as storms, [52]

| Degree of urbanisation | SAIDI |
|---|---|
| rural | $45.51 \frac{min}{yr}$ |
| intermediate | $18.25 \frac{min}{yr}$ |
| urban | $15.75 \frac{min}{yr}$ |

Analysis methods such as the Pareto-principle are very helpful tools to find the most purposeful investment strategies. In order to identify those equipment parts, whose refurbishment has the biggest impact on the overall reliability, all of them are given proportional to their effect on the load-based reliability index ASIDI. A ranking in terms of non-availability is less useful, as some particular unreliable network sections supply negligibly small loads.[48]

This approach can easily be adapted for the improvement of earth fault detection, allowing the detailed locating to help avoiding penalty payments. By thorough analysis those sections are identified, whose upgrade in earth fault detection ensures the biggest benefit for the restoration of supply and therefore on the overall network reliability.

### 6.4.1 The Q-Element and its Impact Factors

The author's premise, that the rate of cross-country faults and their restoration time significantly impact on the Q-Element is researched in this section. In order to find the strongest influences, a sensitivity analysis for a standard network is made.

**Sensitivity Analysis**

The network given in Figure 40 is assumed to be an aged medium voltage cable network consisting of 80 km of cable. Each branch provides e.g. 1.5 MW via 10 km of cable. The earth fault rate is considered to be $3\frac{e/f}{80km \cdot yr}$. For the sensitivity analysis of the Q-Element interruption costs for 10 years of operation are calculated. In order to find the impact of each factor in the calculation of the Q-Element independently from the network's hard-facts (e.g. system length, transformer load installed, fault rate, etc.) they are varied.
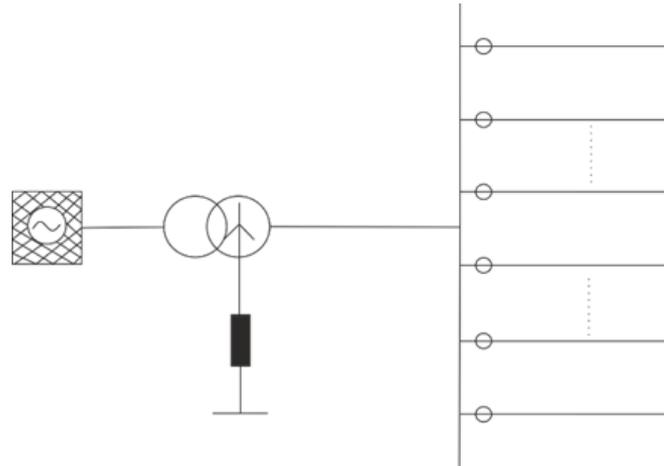
Figure 40: Network structure for the sensitivity analysis of the Q-Element, as shown in the course of the presentation of [4]

Simplifying assumptions for the analysis of continued operation:

- earth faults occur in the front section of the feeder, therefore the whole feeder is interrupted for restoration measures
- fifty percent of the earth faults develop into cross-country faults
- the restoration of cross-country faults takes twice as long, as the restoration of single earth faults

Assumptions for the analysis of immediate tripping combined with improved earth fault detection method:

- earth faults occur in the front section of the feeder, therefore the whole feeder is interrupted for restoration measures
- cross-country faults don't occur due to fast tripping of the faulty branch
- earth fault detection takes 67 % of the original detection time
- value of lost load is $10.6\frac{€}{kWh}$

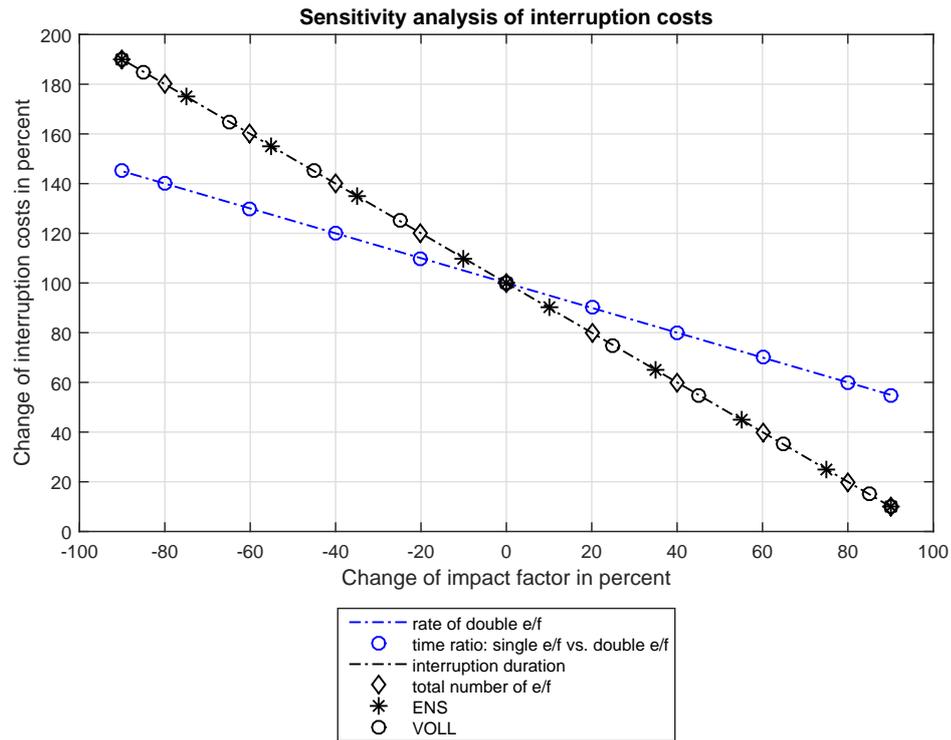The sensitivity to the impact factors is illustrated in Figure 41.

Figure 41: Sensitivity analysis of interruption costs

The impact factors analysed are:

- rate of double earth faults: percentage of single earth faults developing into double earth faults

- time ratio: ratio between the interruption duration of double earth faults and the interruption duration of single earth faults

- interruption duration of single earth faults

- total number of earth faults (including double earth faults)

- energy not supplied caused by earth fault induced interruptions (for the analysis the interrupted load was varied)

- value of lost load

The costs of interruptions due to earth faults are calculated according to Equation 58. Equation 58 is modified to show the dependencies of the interruption costs of single and double earth faults and their respective restoration times - see Equation 59.

$$C = VOLL \cdot P_{interr.} \cdot t_{interr.} \tag{58}$$

$$C = VOLL \cdot P_{interr.} \cdot n_{e/f} \cdot t_{interr.,single} \cdot \left(1 + r_{double,e/f} \cdot f_{t,double,e/f}\right) \tag{59}$$

| $VOLL$ | value of lost load |
|---|---|
| $P_{interr.}$ | interrupted load |
| $t_{interr.}$ | interruption duration |
| $n_{e/f}$ | total number of earth faults |
| $t_{interr.,single}$ | interruption duration of single earth faults |
| $r_{double,e/f}$ | double earth fault rate (e.g. percentage of earth faults that develope into cross-country faults) |
| $f_{t,doublee/f}$ | time factor of double earth faults compared to single earth faults |

While this example works well for sensitivity analysis, it is not necessarily representative for Austrian urban medium voltage networks. Two of the main structural differences are:

- partly meshed network structure, which provides a higher degree of switching options to reach restoration of energy supply.

- automated switching options (e.g. CB), which considerably decrease restoration time ([15] provides an optimisation for distribution automation).

### 6.4.2   Conclusions from the Sensibility Analysis concerning the Impact Factors

The assessment concerning the Q-Element itself and its major impact factors result in the conclusion, that the actual rate of cross-country faults as well as the significant difference in restoration time between earth faults and cross-country faults are not as crucial as assumed (by the author). Sensitivity analyses by means of the example network given in Figure 40 show, that the main factors influencing the Q-Element are the $VOLL$, the total number of earth faults and the restoration time for single line-to-ground faults as well as the interrupted load. The reduction of the total number of earth fault by preventing double earth faults in the first place is an efficient measure, provided the latter occur frequently.

ELECTRICAL
POWER SYSTEMS
TU GRAZ

TU Graz

# 7    Conclusions

In aged medium voltage cable networks, well-established planning and operating principles are questioned, as equipment parts lose dielectric strength. In section 2.2 exemplary damage rates for cables and cable accessories are summarised in order to give an impression on the extents to expect.

If multiple earth faults due to aged cable structures become an issue, the system neutral treatment (earth fault treatment respectively) can be re-evaluated. In section 2.3.1 a process chart is provided, to guide through the decision process.

section 4 contains established earth fault protection methods and the respective design process. In a focussed analysis of the thermic conditions for system neutral resistors used for high detection current methods, an engineering approach to the assessment of thermic stress is presented, which allows a sensible choice of the resistor's lag time. A comparison of the already implemented systems implies, that the used model provides sufficient detail for pre-evaluations.

Concerning incentive based regulatory regimes, all aspects of network reliability gain additional relevance. As many earth fault detection and localisation methods require only little extra effort - equipment and cost-wise - a revised earth fault protection structure allows noticeable improvements at a reasonable expense.

The reduction of cross-country faults by the means of system neutral treatment not only ensures a decrease of interruption duration, but also a noteworthy improvement concerning the interruption frequency. Depending on network specifics, also the earth fault induced non-availability can be decreased considerably. Depending on the networks structure - e.g. switching options, degree of automation, etc. - the load-weighted system average of non-availability (ASIDI) is impacted as well. Furthermore the stress on aged cables and cable accessories such as joints is significantly reduced, enabling even longer life cycles.

Even though a software-based analysis of the influence of single and multiple earth faults on the system availability does not lead to the anticipated results, a reduction of the problem to basic fault scenarios allows representative estimations. As shown in section 6.2 the non-availability changes proportional to its respective impact factors. All graphs show a strictly linear course.

The risk assessment concerning personal safety is a central question in system neutral treatment. One major impact factor is the grounding system itself. In urban cable network structures, a global earthing system can be presumed, allowing high earth fault detection currents. Still thorough analysis and measurement based determination are an absolute necessity.

Elisabeth Hufnagl                                                                                           100

# 8    Appendix

## 8.1    Derivation of Positive Sequence Impedance and Zero Sequence Impedance from Mutual and Self Impedance
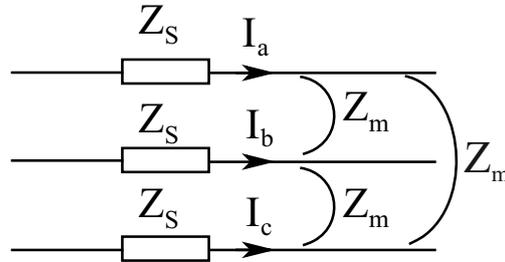


Figure 42: self and mutual impedance of a three phase system

1. Consider the system given in Figure 42 in the positive sequence system:

   – The voltage $V_a$ can be described as $V_a = I_a \cdot Z_s + (I_b + I_c) \cdot Z_m$.

   – As everything is perfectly symmetric $(I_0 = 0)$ $I_a + I_b + I_c = 0$ must apply. As a result the sum of $I_b$ and $I_c$ equals $-I_a$.

   – Therefore $V_a = I_a \cdot (Z_s - Z_m)$.

   – In the positive sequence system the equation $\dfrac{V_1}{I_1} = Z_1 = Z_s - Z_m$ applies.

2. Now consider the system in Figure 42 in the zero sequence system:

   – The fault current $I_F$ equals $(I_a + I_b + I_c)$.

   – As there is no phase shift between those three currents - condition of the zero sequence system, $(I_a + I_b + I_c) = I_a + 2 \cdot I_a$.

   – Now $V_a$ can be described as $(I_a \cdot Z_s + 2 \cdot I_a \cdot Z_m)$.

   – Therefore $V_a = I_a \cdot (Z_s + 2 \cdot Z_m)$.

   – In the zero sequence system the equation $\dfrac{V_0}{I_0} = Z_s + 2 \cdot Z_m$ applies.

## 8.2 Calculation Details

| Network characteristics | |
|---|---|
| $H_{e/f}$ | $0.77 \; \dfrac{1}{100km \cdot yr}$ |
| $r_{double,e/f}$ | 0.5 |
| feeder length | 10 km |
| system length | 80 km |

Table 11: Network specifications

| Interruption durations (starting values) | |
|---|---|
| $d_1$ | 10 minutes |
| $d_{1,d-e/f}$ | 1 hour |
| $d_2$ | 2 hours |
| $d_3$ | 2 hours |
| $d_4$ | 2 hours |

Table 12: Starting values for interruption durations

# References

[1] F. Javernik, E. Hufnagl, M. Aigner, and E. Schmautzer, "The compliant integration of (renewable) power sources in MV or LV grids and the impact on grid reliability," in *2015 International Conference on Renewable Energy Research and Applications (ICRERA)*, pp. 536–541, Nov 2015.

[2] E. Hufnagl, M. Aigner, and E. Schmautzer, *Evaluation of an urban medium-voltage network by using reliability indices.* No. 83(1-2) in ELEK-TROTEHNIŠKI VESTNIK, Journal of Electrical Engineering and Computer Science, 2016.

[3] E. Hufnagl, L. Fickert, and E. Schmautzer, *A simplified procedure to determine the earth-fault currents in compensated networks.* No. 83(3) in ELEK-TROTEHNIŠKI VESTNIK, Journal of Electrical Engineering and Computer Science, 2016.

[4] E. Hufnagl and L. Fickert, *Erdschlussbehandlung unter regulatorischen Aspekten.* ETG-Fachbericht 151, VDE-Verlag, 2017.

[5] S. Schmidt and A. Milbich, *Umstellung eines Netzes auf NOSPE-Betriebserfahrungen am Beispiel des 20-kV-Netzes der Stadtwerke Karlsruhe Netzservice.* ETG-Fachbericht 151, VDE-Verlag, 2017.

[6] M. Worch and S. Schmidt, *Umstellung eines Netzes auf NOSPE-Gründe und Randbedingungen am Beispiel des 20-kV-Netzes der Stadtwerke Karlsruhe Netze.* ETG-Fachbericht 129, VDE-Verlag, 2011.

[7] O. Siirto, M. Loukkalahti, M. Hyvärinen, P. Heine, and M. Lehtonen, "Neutral point treatment and earth fault suppression," in *2012 Electric Power Quality and Supply Reliability*, pp. 1–6, June 2012.

[8] G. Achleitner, "Earth Fault Distance Protection," Doctoral Dissertation, Graz University of Technology, 2008.

[9] G. Druml, "Innovative Methoden zur Erdschlussortung und Petersen-Spulen Regelung," Doctoral Dissertation, Graz University of Technology, 2012.

[10] M. Loos, "Single Phase to Ground Fault Detection and Location in Compensated Network," Doctoral Dissertation, Brussels School of Engineering, 2014.

[11] C. Obkircher, "Ausbaugrenzen gelöscht betriebener Netze," Doctoral Dissertation, Graz University of Technology, 2008.

[12] E. Fuchs, "Kritische Betrachtung des Löschverhaltens in kompensierten 20-kV-Netzen - Auswertung von alten und neuen Erdschlussdaten," Doctoral Dissertation, Graz University of Technology, 2013.

[13] D. Topolánek, J. Orságová, J. Dvořák, and P. Toman, "The method of the additional earthing of the affected phase during an earth fault and its influence on MV network safety," in *2011 IEEE Trondheim PowerTech*, pp. 1–8, June 2011.

[14] e-control, "Trassen- und Systemlängen zum 31. Dezember 2016," 2016. `https://www.e-control.at/statistik/strom/bestandsstatistik`; (visited on June 7th 2018).

[15] O. Siirto, "Distribution Automation and Self-Healing Urban Medium Voltage Networks," Doctoral Dissertation, Aalto University, 2016.

[16] J. Bühler, M. Hallas, and G. Balzer, "Risikoorientierte Instandhaltungsoptimierung von Mittelspannungskabeln," 2012. 12.Symposium Energieinnovation.

[17] Forschungsgemeinschaft für Elektrische Anlagen und Stromwirtschaft e.V. (FGH), "Technischer Bericht 299: Asset-Management von Verteilungsnetzen - Komponentenverhalten und Analyse des Kostenrisikos," 2006.

[18] O. Siirto, J. Vepsäläinen, A. Hämäläinen, and M. Loukkalahti, "Improving reliability by focusing on the quality and condition of medium-voltage cables and cable accessories," *CIRED - Open Access Proceedings Journal*, vol. 2017, no. 1, pp. 229–232, 2017.

[19] J. Z. Hansen, "Results from Danish failure statistics for medium voltage XLPE cables," in *22nd International Conference and Exhibition on Electricity Distribution (CIRED 2013)*, pp. 1–4, June 2013.

[20] E. Maggioli, H. Leite, and C. Morais, "A survey of the Portuguese MV underground cable failure," in *2016 13th International Conference on the European Energy Market (EEM)*, pp. 1–5, June 2016.

[21] F. Williams, "Cable accessory failure analysis," 2010. ICC Educational Session (NEETRAC Publications), Georgia, USA.

[22] R. Hartlein, N. Hampon, and J. Perkel, "Diagnostic testing of underground cable systems," 2010. ICC Educational Session (NEETRAC Publications), Georgia, USA.

[23] Y. He and Elforsk, *Study and Analysis of Distribution Equipment Reliability Data.* Elforsk rapport, Elforsk, 2010.

[24] T. Mallits, "Fehlerstromaufteilung und Potentialverhältnisse in verbunden (Globalen-) Erdungssystemen," Doctoral Dissertation, Graz University of Technology, 2018.

[25] E. Hufnagl, "Einfluss von Umstrukturierungsmaßnahmen auf die Zuverlässigkeitskennzahlen in einem städtischen Mittelspannungsnetz," Master Thesis, Technische Universität Graz, 2014.

[26] "IEEE Guide for Electric Power Distribution Reliability Indices," *IEEE Std 1366-2012 (Revision of IEEE Std 1366-2003)*, pp. 1–43, May 2012.

[27] BCP BUSARELLO + COTT + PARTNER AG, *NEPLAN User's Guide V5.*

[28] H. Renner and M. Sakulin, "Spannungsqualität und Versorgungszuverlässigkeit," vorlesungsskript, Institut für Elektrische Anlagen, Technische Universität Graz, 2008.

[29] H. Nagel, *Systematische Netzplanung.* Anlagentechnik für elektrische Verteilungsnetze, VDE-Verlag, 2008.

[30] Forum Netztechnik/Netzbetrieb im VDE, "Störungs- und Verfügbarkeitsstatistik," 2017.

[31] H. Vennegeerts, C. Schröders, M. Holthausen, D. Quadflieg, and A. Moser, "Ermittlung von Eingangsdaten zur Zuverlässigkeitsberechnung aus der FNN-Störungsstatistik," 2013. `http://www.fgh.rwth-aachen.de/verein/publikat/veroeff/FGH_IAEW_Eingangsdaten_Zuverlaessigkeitsberechnung_2013.pdf`; (aufgerufen am 10. September 2014).

[32] W. Rischawy, "Technische Anwendbarkeit und wirtschaftliche Bewertungsfaktoren von Erdschlussortungsverfahren in städtischen Mittelspannungsnetzen," Master Thesis, Graz University of Technology, 2015.

[33] L. Fickert, "Schutz und Versorgungssicherheit elektrischer Energiesysteme," lecture Material, Institute of Electrical Power Systems, Graz University of Technology, 2005.

[34] Fickert, L., "Research Seminar (Privatissimum: Lothar Fickert, Elisabeth Hufnagl) ." Oral notice Em.Univ.-Prof. Dipl.-Ing. Dr.techn. Lothar Fickert.

[35] L. Fickert, "Technical Application and Economic Assessment Factors of different Earth Fault Detection Methods in Medium Voltage Networks," 2016. International Scientific Conference on Electric Power Engineering (EPE).

[36] CENELEC, "Erdung von Starkstromanlagen mit Nennwechselspannungen über 1 kV; EN 50522," 2010.

[37] H. Steurer, L. Fickert, and E. Schmautzer, "Einführung eines neuen Erdschlussortungs-Systems KNOPE und erste Erfahrungen," *e & i Elektrotechnik und Informationstechnik*, vol. 131, pp. 289–296, Dec 2014.

[38] C. L. Fortescue, "Method of symmetrical co-ordinates applied to the solution of polyphase networks," June 1918. Presented at the 34th annual convention of the American Institute of Electrical Engineers, Atlantic City.

[39] G. Verfahrenstechnik und Chemieingenieurwesen and Verein Deutscher Ingenieure, *VDI-Wärmeatlas*. VDI-Wärmeatlas, Springer Berlin Heidelberg, 2013.

[40] W. Wagner, *Wärmeübertragung: Grundlagen*. Kamprath-Reihe, Vogel, 2004.

[41] FRITZLEN POWER RESISTORS, "Dynamics Through Resistance." `http://www.frizlen.com/de/service/download/?tx_maritfaldownloads_list%5Baction%5D=list&tx_maritfaldownloads_list%5Bcontroller%5D=File`; (visited on March 21st 2018).

[42] M. Humayun, "Demand Response Benefits for Major Assets of high Voltage Distribution Systems," Doctoral Dissertation, Aalto University, 2015.

[43] M. Lindinger, "Nachweis globaler Erdungssysteme durch Messung und Berechnung von verteilten Erdungsanlagen," Doctoral Dissertation, Graz University of Technology, 2012.

[44] T. Mallits, "Die Rolle von Globalen Erdungssystemen zur Sicherstellung der Zuverlässigkeit elektrischer Netze," 2016. 14.Symposium Energieinnovation.

[45] Energy Networks Association Limited, "EG-0 Power System Earthing Guide Part 1: Management Principles, Version 1," 2010.

[46] I. Griffiths, D. J. Woodhouse, and B. Pawlik, "What are the chances of that? A primer on probability and poisson processes for earthing designers," in *2016 Down to Earth Conference (DTEC)*, pp. 1–6, Sept 2016.

[47] CONSENTEC GmbH, "Gutachten zur Einführung einer Qualitätsregulierung für österreichische Stromnetzbetreiber zur dritten Anreizregulierungsperiode," 2013.

[48] A. Lipp, "Entwicklung einer Verkabelungsstrategie für ein Verteilernetz," Master Thesis, Technische Universität Graz, 2016.

[49] CONSENTEC GmbH, "Konzeptionierung und Ausgestaltung eines Qualitäts-Elements (Q-Element) im Bereich Netzzuverlässigkeit Strom sowie dessen Integration in die Erlösobergrenze," 2010.

[50] U. Rührnößl and R. Görlich, "Optionen zur Einbeziehung der Versorgungsqualität in derzeitige bzw. künftige Regulierungsrahmen für Stromverteilernetzbetreiber," 2014.

[51] e-control, "Ausfall- und Störungsstatistik für Österreich," 2017. `https://www.e-control.at/documents/20903/388512/Ausfall-+` `und+St%C3%B6rungsstatistik+f%C3%BCr+%C3%96sterreich.pdf/` `21b52a6d-431e-c9ed-f951-c6d54dd19ac8;` (visited on May 4th 2018).

[52] e-control, "Ausfall- und Störungsstatistik für Österreich," 2016. `https://www.e-control.at/documents/20903/388512/Ausfall-+` `und+Stoerungsstatistik+2015_Stromausfallsdauer_E-Control.pdf/` `7f8bd3ae-951f-45e7-a6d2-a791ed7872e8;` (visited on May 4th 2018).